Article

Cell Reports

Mycobacterium smegmatis HtrA Blocks the Toxic Activity of a Putative Cell Wall Amidase

Graphical Abstract

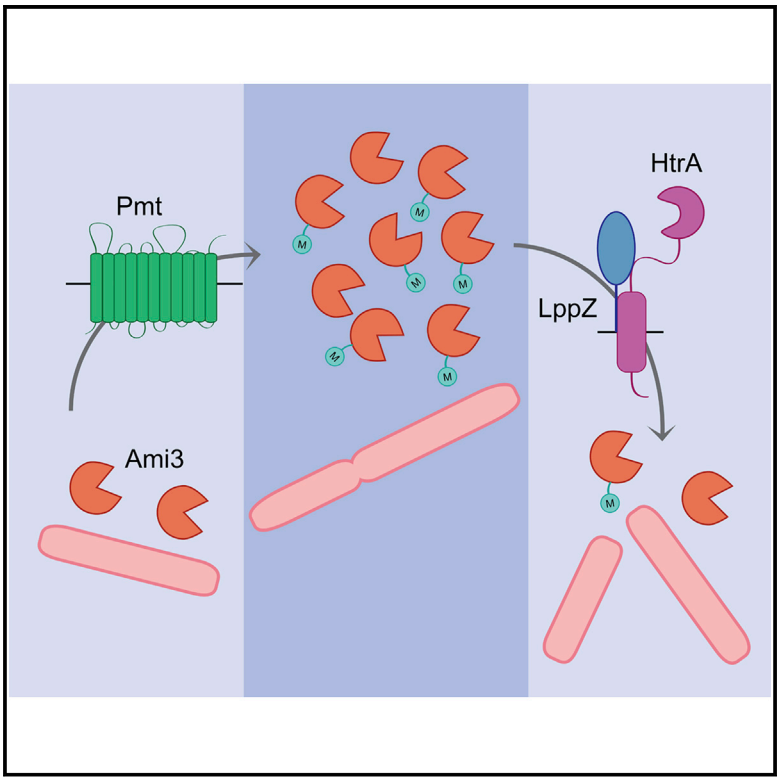

Authors

Katherine J. Wu, Cara C. Boutte, Thomas R. Ioerger, Eric J. Rubin

Correspondence

erubin@hsph.harvard.edu

In Brief

Wu et al. show that in *Mycobacterium smegmatis*, the putative cell wall amidase Ami3 can accumulate to toxicity under the stabilizing influence of Pmt mannosylation. To control Ami3 levels, an essential complex between the periplasmic serine protease HtrA and the lipoprotein LppZ regulates Ami3 levels, maintaining cellular integrity.

Highlights

- HtrA-LppZ is an essential protease-lipoprotein complex in *Mycobacterium smegmatis*
- HtrA-LppZ is required to negatively regulate Ami3, a putative cell wall amidase
- Without HtrA-LppZ, Ami3 can accumulate to toxicity when mannosylated by Pmt

Wu et al., 2019, Cell Reports *27*, 2468–2479
May 21, 2019
https://doi.org/10.1016/j.celrep.2018.12.063

CellPress

OPEN ACCESS
CellPress

Cell Reports
Article

Mycobacterium smegmatis HtrA Blocks the Toxic Activity of a Putative Cell Wall Amidase

Katherine J. Wu,[1] Cara C. Boutte,[2] Thomas R. Ioerger,[3] and Eric J. Rubin[1,4,*]
[1]Department of Immunology and Infectious Diseases, Harvard T.H. Chan School of Public Health, Boston, MA 02115, USA
[2]Department of Biology, University of Texas at Arlington, Arlington, TX 76019, USA
[3]Department of Computer Science, Texas A&M University, College Station, TX 77843, USA
[4]Lead Contact
*Correspondence: erubin@hsph.harvard.edu
https://doi.org/10.1016/j.celrep.2018.12.063

SUMMARY

***Mycobacterium tuberculosis*, the causative agent of tuberculosis, withstands diverse environmental stresses in the host. The periplasmic protease HtrA is required only to survive extreme conditions in most bacteria but is predicted to be essential for normal growth in mycobacteria. We confirm that HtrA is indeed essential in *Mycobacterium smegmatis* and interacts with another essential protein of unknown function, LppZ. However, the loss of any of three unlinked genes, including those encoding Ami3, a peptidoglycan muramidase, and Pmt, a mannosyltransferase, suppresses the essentiality of both HtrA and LppZ, indicating the functional relevance of these genes' protein products. Our data indicate that HtrA-LppZ is required to counteract the accumulation of active Ami3, which is toxic under the stabilizing influence of Pmt-based mannosylation. This suggests that HtrA-LppZ blocks the toxicity of a cell wall enzyme to maintain mycobacterial homeostasis.**

INTRODUCTION

Mycobacterium tuberculosis (*Mtb*), the causative agent of tuberculosis, remains the greatest infectious killer in human history, claiming 1.5 million lives each year (World Health Organization, 2017). Despite this enormous public health burden, efforts to curb *Mtb*'s spread and prevent rising rates of drug resistance have stagnated in recent decades. To combat the extremes of host defenses, *Mtb* deploys a tightly controlled array of stress response systems, including a large number of proteases. Recently mycobacterial proteases have emerged as appealing therapeutic targets because several of the most conserved homologs, including Clp, FtsH, HtrA, and the proteasome, are essential for the growth or virulence of *Mtb* (Raju et al., 2012a).

Despite their integral role in *Mtb* cell biology, mycobacterial proteases remain understudied. Recent work in our lab has implicated the mycobacterial Clp protease in the turnover of the essential transcriptional repressor WhiB1 (Raju et al., 2012b, 2014). Similarly, transposon insertion sequencing data have indicated that the periplasmic serine protease HtrA (MSMEG_5070, Rv1223) is essential in mycobacteria (Griffin et al., 2011; Zhang et al., 2012; DeJesus and Ioerger, 2013). Despite this, the reasons for HtrA's essentiality have remained unclear.

In *E. coli* and other organisms, HtrA is characterized as a non-essential, periplasmic protease with secondary chaperone function (Clausen et al., 2011). Although dispensable for normal growth, HtrA is crucial for the virulence of several intracellular pathogens, including *Shigella*, *Listeria*, and *Salmonella* (Ingmer and Brøndsted, 2009). In these species, HtrA is required to tolerate a common set of stressful conditions, including high temperature, oxidative stress, and macrophage survival. The well-characterized *E. coli* HtrA homolog DegP is induced in conditions of membrane stress and becomes essential during heat shock (Ingmer and Brøndsted, 2009). DegP contains a protease domain with a conserved Ser-His-Asp catalytic triad and two PDZ domains (Figure 1A) that regulate substrate binding and access to the proteolytic chamber. Although a handful of substrates have been identified in *E. coli* (Clausen et al., 2002), DegP appears to be mostly indiscriminate in its specificity, preferring denatured, unfolded substrates with hydrophobic C termini.

Like *E. coli* and many other organisms, virulent mycobacteria express three orthologs of HtrA. In *Mtb*, these are *htrA* (Rv1223), *htrA2*/*pepD* (Rv0983), and *htrA3*/*pepA* (Rv0125); of these, only HtrA is predicted to be essential. However, this essentiality appears to be conserved across all mycobacteria, regardless of pathogenicity, including in the fast growing *Mycobacterium smegmatis* (*Msm*), which encodes both *htrA* (MSMEG_5070) and the non-essential *pepD* (MSMEG_5486) (Lew et al., 2011). Nevertheless, *htrA*'s synteny in mycobacteria indicates that its transcription may be stress responsive, as it lies in an operon with *sigE*, a stress-responsive alternative sigma factor (Manganelli et al., 2004). Additionally, its high degree of sequence conservation with homologs in other species indicates that HtrA may be capable of recapitulating some stress-responsive or virulence functions. Although HtrA's role in mediating the mycobacterial stress response may partially overlap with its homologs in other species, its essentiality indicates it must be involved in a unique regulatory pathway that supports mycobacterial growth and survival.

Here, we present evidence that HtrA serves a previously undescribed and essential role in the regulation of the growth of *Msm* by degrading a putative cell wall muramidase. HtrA engages in a periplasmic complex with another essential protein, LppZ, to control levels of the lethal hyperactivity of Ami3, an amidase

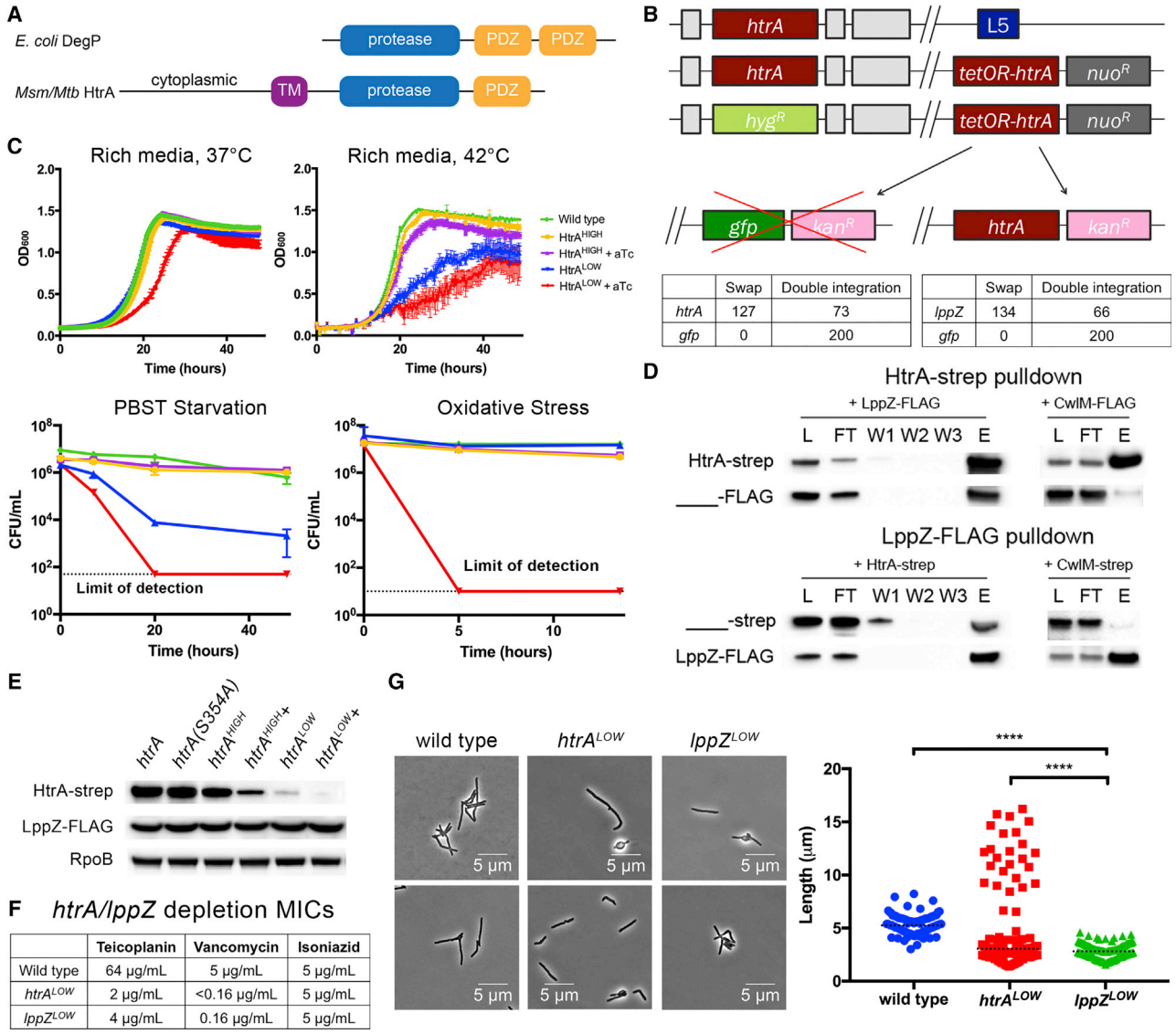

F *htrA/lppZ* depletion MICs

	Teicoplanin	Vancomycin	Isoniazid
Wild type	64 µg/mL	5 µg/mL	5 µg/mL
htrA^{LOW}	2 µg/mL	<0.16 µg/mL	5 µg/mL
lppZ^{LOW}	4 µg/mL	0.16 µg/mL	5 µg/mL

	Swap	Double integration
htrA	127	73
gfp	0	200

	Swap	Double integration
lppZ	134	66
gfp	0	200

Figure 1. HtrA-LppZ Are Essential Interacting Proteins in *Mycobacterium smegmatis*

(A) DegP/HtrA homolog domain architecture. *E. coli* DegP contains a protease domain and two C-terminal PDZ domains. In contrast, mycobacterial HtrA is anchored in the inner membrane and contains a single PDZ domain. Additionally, mycobacterial HtrA has a cytoplasmic domain with no homology to any known protein.

(B) HtrA and LppZ are essential by L5 swap. Top: a schematic of the L5 essentiality swap. Placing a second copy of *htrA*, along with a nourseothricin resistance cassette, at the L5 phage integration site allows replacement of endogenous *htrA* with a hygromycin resistance cassette. This copy of *htrA* can be swapped for another copy of *htrA* with a different antibiotic resistance marker but not for a functionally unrelated gene such as *gfp*. Bottom: quantification of *htrA* and *gfp* swaps. A total of 200 transformants were tested for antibiotic resistance. An equivalent swap was performed for *lppZ* and enumerated in the same manner.

(C) Cells depleted of HtrA grow at a slower rate. When regulated by an aTc-repressible promoter, *htrA* can be transcriptionally depleted from cells. Two strains were constructed: *htrA*^{HIGH}, which used a strong promoter susceptible to aTc-based repression, and *htrA*^{LOW}, a weak promoter susceptible to aTc-based repression. These strains were grown, with or without aTc, in each of four conditions: rich media at 37°C, high temperature (42°C), carbon-nitrogen starvation (PBS-Tween 20), and oxidative stress (0.02% tert-butyl hydroperoxide). Error bars represent SD of the mean.

(D) HtrA and LppZ interact. HtrA-Strep and LppZ-FLAG were individually immunoprecipitated using anti-Strep and anti-FLAG magnetic beads, respectively, and the following fractions were analyzed using western blotting: L, lysate; FT, flow through; W1, wash 1; W2, wash 2; W3, wash 3; and E, elution. Control immunoprecipitations lacking the respective bait were performed simultaneously and lysate, flow through, and elution were analyzed.

(E) LppZ is not a substrate of HtrA. Strains expressing *htrA* or *htrA(S354A)* under *htrA*'s native promoter, *htrA*^{HIGH}, or *htrA*^{LOW} were grown to log phase, and cell lysate was analyzed using western blotting to detect levels of HtrA-Strep and LppZ-FLAG. In the case of *htrA*^{HIGH} and *htrA*^{LOW}, strains were also grown with or without 100 ng/mL aTc.

(legend continued on next page)

stabilized by Pmt-mediated O-mannosylation. Loss of either *ami3* or *pmt* is sufficient to relieve the essentiality of both *htrA* and *lppZ*. These data expand upon a growing body of literature illustrating the complex ways in which bacteria regulate growth and division.

RESULTS

HtrA-LppZ Forms an Essential Complex in the Mycobacterial Periplasm

Previous transposon insertion-based (Tn-seq) screens have predicted the essentiality of *htrA* in both *Msm* and *Mtb* (Griffin et al., 2011; Zhang et al., 2012; DeJesus and Ioerger, 2013). To confirm *htrA* essentiality, we attempted to delete these genes from the genome of *M. smegmatis* through mycobacterial recombineering and homologous recombination (Figure 1B, top). Briefly, a second copy of *htrA* was transformed into the L5 phage integration site with a nourseothricin resistance cassette, allowing the replacement of the endogenous copy of *htrA* with a hygromycin resistance cassette. We then attempted to transform *htrA* or an empty vector with a kanamycin resistance cassette into the L5 integration site (an "L5 swap"). Three outcomes can result from these experiments. First, integrations resulting in nonviable cells will prevent the growth of transformants on antibiotic selection. Second, successful "swaps" are those that acquire kanamycin resistance at the expense of nourseothricin resistance, indicating the replacement of the original integrated vector with the transformed vector. Third, the second vector may recombine in alongside the original vector, creating a double integrant that retains resistance to both antibiotics. In these experiments, *htrA* swapped in at a rate of 63.5%, while the empty vector yielded only double integrants (Figure 1B, bottom), indicating that HtrA is essential.

To assess the phenotype of *htrA* hypomorphs, we constructed depletion strains in which the only copies of *htrA* were under the control of anhydrotetracycline (aTc)-repressible promoters of different strengths ($htrA^{LOW}$ and $htrA^{HIGH}$). With the addition of aTc, $HtrA^{LOW}$ cells clumped in liquid culture and exhibited a slower growth rate (Figure 1C) but remained viable, suggesting that a minimal amount of HtrA is sufficient to sustain growth. As HtrA homologs in other bacterial species are associated with protection against environmental stress, we tested the ability of depleted $htrA^{LOW}$ cells to survive extreme conditions, including high temperature, oxidative stress, and carbon-nitrogen starvation (Figure 1C). All tested conditions impaired the growth of or killed depleted $htrA^{LOW}$ cells, indicating that higher amounts of HtrA are required to sustain growth under environmental stress.

We reasoned that identifying binding partners could help define HtrA's function. To find interactors, we immunoprecipitated Strep-tagged HtrA and identified eluted proteins using mass spectrometry. The most abundant protein, LppZ (MSMEG_2369, Rv3006), had no known function. LppZ is also predicted to be essential in both *M. smegmatis* and *M. tuberculosis* and is annotated as a putative secreted lipoprotein (Griffin et al., 2011; Zhang et al., 2012; DeJesus and Ioerger, 2013). We confirmed LppZ essentiality with an L5 swap (Figure 1B) and detected a stable interaction between HtrA and LppZ by co-immunoprecipitation of tagged proteins (Figure 1D).

On the basis of this interaction, LppZ could be an HtrA substrate or adaptor. To distinguish between these possibilities, we tagged LppZ with a FLAG sequence and monitored its stability during depletion of *htrA*. LppZ levels were completely insensitive to alterations in HtrA (Figure 1E). This suggests that LppZ may be an adaptor of HtrA proteolytic activity, analogous to interactions in *E. coli* between the periplasmic protease Prc and the lipoprotein NlpI (Singh et al., 2015; Tadokoro et al., 2004) and between DegP and recombinant mutants of the lipoprotein Lpp (Park et al., 2017).

If LppZ is an HtrA adaptor, LppZ mutants should phenocopy HtrA mutants. Indeed, both $htrA^{LOW}$ and $lppZ^{LOW}$ depletion strains exhibited increased sensitivity to antibiotics targeting cell wall crosslinking (but not other antibiotics such as isoniazid) (Figure 1F) and severe morphological defects (Figure 1G). Cells bulged and shortened upon $htrA^{LOW}$ or $lppZ^{LOW}$ depletion; however, a small subpopulation branched in only the $htrA^{LOW}$ depletion. Both these morphologies are reminiscent of previously characterized strains in which dysregulation of cell wall machinery induces swelling and branching (Chao et al., 2013; Kieser et al., 2015). These data suggest that HtrA and LppZ act cooperatively as a complex in the same step of an essential genetic pathway that engages the cell wall.

Loss-of-Function Mutations in *ami3*, *pmt*, or *mprB* Suppress *htrA* and *lppZ* Essentiality

Unlike *E. coli* DegP, mycobacterial HtrA is predicted to be membrane anchored and have only one PDZ domain. Furthermore, it has a unique cytoplasmic domain at its N terminus that bears no homology to any known protein (Kapopoulou et al., 2011). To understand structure-function relationships in HtrA, we made a series of domain deletions and tested their viability using L5 swaps. We found that both the cytoplasmic and PDZ domains are essential for function (Figure S1A) but do not affect HtrA's interaction with LppZ (Figure S1B). However, these experiments yielded a small number of survivors that grew despite loss of functional HtrA. We hypothesized that these might be due to mutations elsewhere in the chromosome and performed whole-genome sequencing of these strains to identify potential extragenic suppressors of *htrA* essentiality.

We sequenced nine strains in total and compared their genomes with that of the parental strains. Each swapped strain carried at least one of the following mutations (Figure S1C):

(F) Cells lacking HtrA or LppZ are highly sensitive to cell wall-targeting antibiotics. $htrA^{LOW}$ and $lppZ^{LOW}$, strains expressing the respective essential gene under a weak promoter susceptible to aTc-based repression, were grown in teicoplanin and vancomycin, antibiotics targeting D-ala-D-ala crosslinking in the mycobacterial cell wall, and isoniazid, an antibiotic that inhibits mycolic acid synthesis.

(G) Depletion of HtrA or LppZ induces morphological defects. $htrA^{LOW}$ and $lppZ^{LOW}$ were grown to log phase in aTc and observed under the microscope. Two representative images for each strain are shown. At least 100 cells were quantified in each condition. Dotted black lines indicate median values. Western blot images were cropped, but display all relevant lanes and reactive bands. ****$p < 0.0001$.

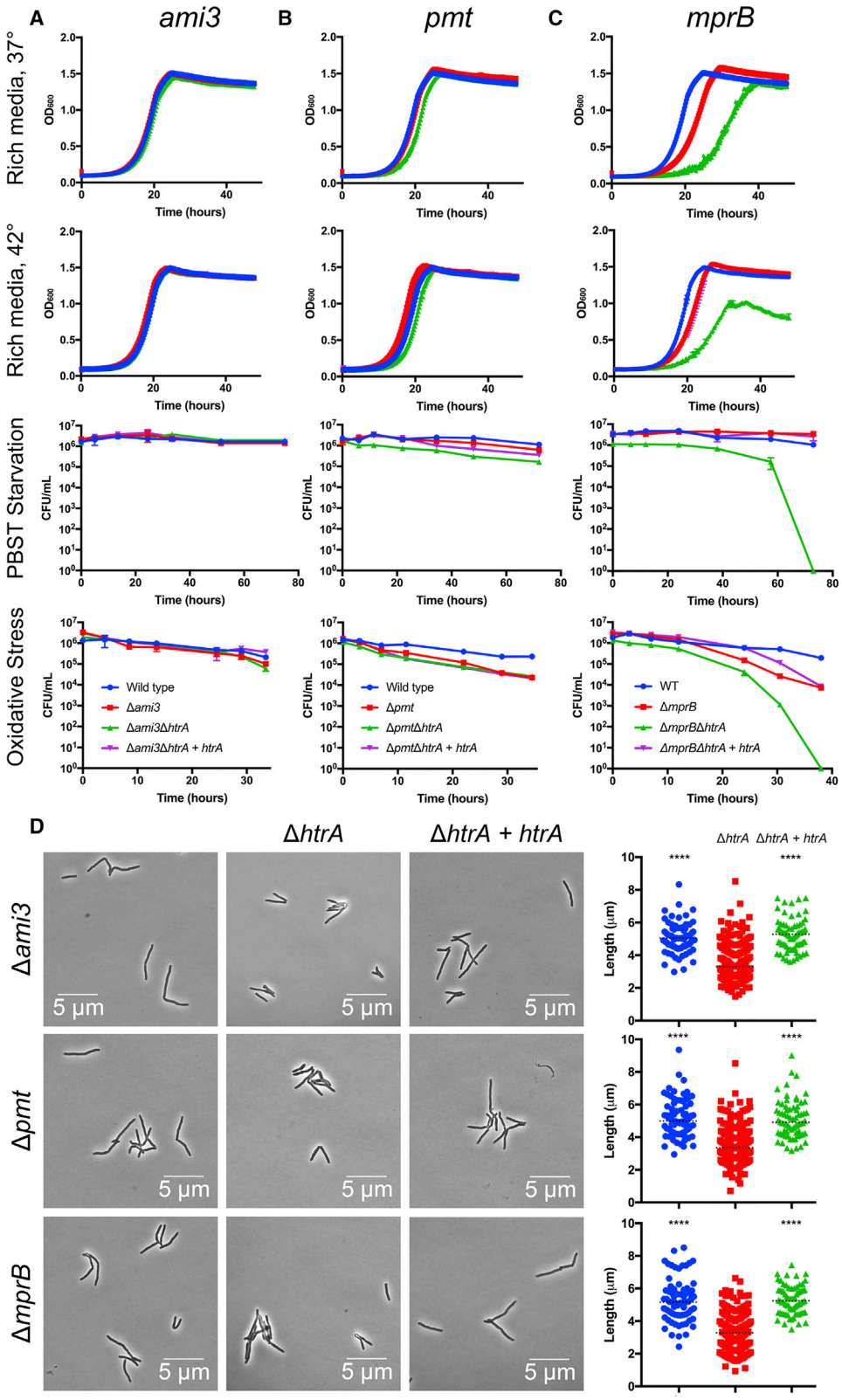

(legend on next page)

one of five different frameshift mutations in *ami3* (MSMEG_6406, or Rv8311 in *Mtb*), a putative N-acetylmuramoyl-L-alanine amidase; a frameshift mutation in *pmt* (MSMEG_5447, or Rv1002c in *Mtb*), a dolichyl-phosphate-mannose-protein mannosyltransferase; or two SNPs in *mprB* (MSMEG_5487, or Rv0982 in *Mtb*), the sensor histidine kinase of a two-component regulatory system that also includes *mprA* (MSMEG_5488, or Rv0981 in *Mtb*). All of these genes are non-essential in *Mtb* and *Msm* (Griffin et al., 2011; Zhang et al., 2012; DeJesus and Ioerger, 2013). To verify these suppressors, we generated double-deletion strains in fresh backgrounds. The Δ*ami3*Δ*htrA* and Δ*pmt*Δ*htrA* double-deletion strains grew robustly under all growth conditions tested, including those in which the $htrA^{LOW}$ depletion strain failed to grow or died (Figures 2A and 2B). However, the Δ*mprB*Δ*htrA* double-deletion strain, although viable, grew slowly even under optimal conditions and remained moderately susceptible to environmental stress (Figure 2C). Importantly, loss of *ami3*, *pmt*, or *mprB* also allowed disruption of the otherwise essential *lppZ* (Figure S2). Given that *mprB* only partially suppresses the essentiality of *htrA*, and the previously characterized, wide-reaching transcriptional effects of deleting *mprB* (He et al., 2006), we focused our subsequent experiments on *ami3* and *pmt*.

Double-deletion strains allowed us to study the growth and morphology of strains that lacked *htrA* and *lppZ*. The suppressed strains grew at near normal rates (Figures 2A–2D), unlike the *htrA* depletion strain. Additionally, Δ*ami3*Δ*htrA* and Δ*ami3*Δ*lppZ* were less sensitive to teicoplanin and vancomycin than the *htrA* and *lppZ* depletions (Figure S2C). However, double-deletion strains in all backgrounds exhibited reduced cell length (Figures 2D, S2A, and S2B), much like the *htrA* and *lppZ* depletions, indicating that the HtrA-LppZ complex may have an additional, non-essential function that affects cell division or elongation.

Ami3 Is Toxic when Overexpressed

Because deletions of *ami3* and *pmt* could independently suppress the essentiality of both *htrA* and *lppZ*, we reasoned that these genes may operate within the same pathway. In *E. coli*, the peptidoglycan endopeptidase MepS has been shown to be negatively regulated by the periplasmic protease Prc in conjunction with a lipoprotein adaptor, NlpI (Schwechheimer et al., 2015; Singh et al., 2015). Because the *htrA* and *lppZ* depletion phenotypes (Figures 1F and 1G) mimic cell wall dysregulation (Chao et al., 2013; Kieser et al., 2015), we hypothesized that the putative cell wall enzyme Ami3 might be a substrate of HtrA-LppZ. Indeed, when expressed under an aTc-inducible promoter (Figure S3A), *ami3* overexpression quickly led to cell death (Figure 3A, top). We found the aTc minimum inhibitory concentration (MIC) of this strain to be about 12 ng/mL. This toxicity was exacerbated at high temperature (Figure 3A, bottom), mirroring the sensitivity of $htrA^{LOW}$ depletion (Figure 1C). Furthermore, cells overexpressing *ami3* exhibited reduced cell length and large polar bulges (Figure 3B), phenocopying *htrA* and *lppZ* depletion (Figure 1G). When C-terminally tagged with mRFP, Ami3 localized to the poles, mid-cell, and bulges, all points of cell growth and division (Figure S3B).

Ami3 exhibits some structural homology to *E. coli* AmiD, a zinc metalloprotease in the amidase_2 domain family of cell wall hydrolyzing amidases (Kelley et al., 2015; Senzani et al., 2017). Threading the Ami3 sequence into the AmiD structure using Phyre2 allowed us to identify a potential triad of zinc-coordinating residues in Ami3 consisting of two histidines (H226, H362) and a cysteine (C370). To test the contribution of Ami3 enzymatic activity to HtrA essentiality, we constructed mutants carrying amino acid substitutions in each of these residues and attempted to swap enzymatically inactive versions of *ami3* into a strain lacking the endogenous copies of both *ami3* and *htrA* and carrying a copy of *htrA* at the L5 integration site. We found that that the inactive alleles could exchange with *htrA* and, in an analogous experiment, *lppZ* (Figure 3C). Thus, HtrA and LppZ are only essential in the presence of Ami3 catalytic activity.

If Ami3 hyperactivity leads to cell death, mutating the catalytic residues of Ami3 might relieve toxicity. Indeed, overexpression of *ami3(H226A)*, *ami3(H362A)*, or *ami3(C370S)* was no longer lethal to cells (Figure 3A). However, full wild-type viability was not restored, indicating that even inactive *ami3* still retains some toxicity despite being expressed at levels broadly similar to the wild-type allele (Figures 3C and S3C). Cells that overexpressed the mutant protein were still abnormal, albeit with a morphology distinct from that of wild-type Ami3 overexpression: overaccumulation of the catalytically inactive mutants of Ami3 resulted in long, branching cells (Figure 3B). These cells resemble a subpopulation of cells with increased length and branching observed upon *htrA* depletion (Figure 1G).

HtrA-LppZ Regulates Ami3

On the basis of the correlation in phenotypes between *ami3* overexpression and *htrA* and *lppZ* depletion, we hypothesized that HtrA-LppZ negatively regulates Ami3. To test this, we constructed strains in which the only copies of *htrA* and *lppZ* were expressed only in the presence of inducer and monitored levels of Ami3.

As expected, Ami3 levels decreased with HtrA induction (Figure 4A). We next mutated the catalytic serine of *htrA*, creating *htrA(S354A)*. In PepD, another mycobacterial HtrA homolog, this mutation ablates up to 90% of proteolytic activity (White et al., 2010, 2011). As expected, Ami3 levels were less affected

Figure 2. Loss-of-Function Mutations in *ami3*, *pmt*, or *mprB* Suppress *htrA* Essentiality

(A–C) Double-mutant phenotypes of *htrA* suppressor strains: *ami3* (A), *pmt* (B), and *mprB* (C). Wild-type *Mycobacterium smegmatis* (*Msm*), single suppressor gene deletions, suppressor deletions with *htrA* deletions, and *htrA* complemented strains (see Figures S1 and S6) were grown under conditions identical to those in Figure 1, including growth in rich media at 37°C, high temperature (42°C), carbon-nitrogen starvation (PBS-Tween 20), and oxidative stress (0.02% tert-butyl hydroperoxide). Error bars represent SD of the mean.

(D) *htrA* suppressor mutants exhibit reduced cell length. Single suppressor deletion strains (blue), *htrA* double-deletion strains (red), and *htrA* complemented strains (green) were grown to log phase and analyzed for total cell length (see Figure S2). At least 70 cells were quantified in each condition. Dotted black lines indicate median values. ****$p < 0.0001$.

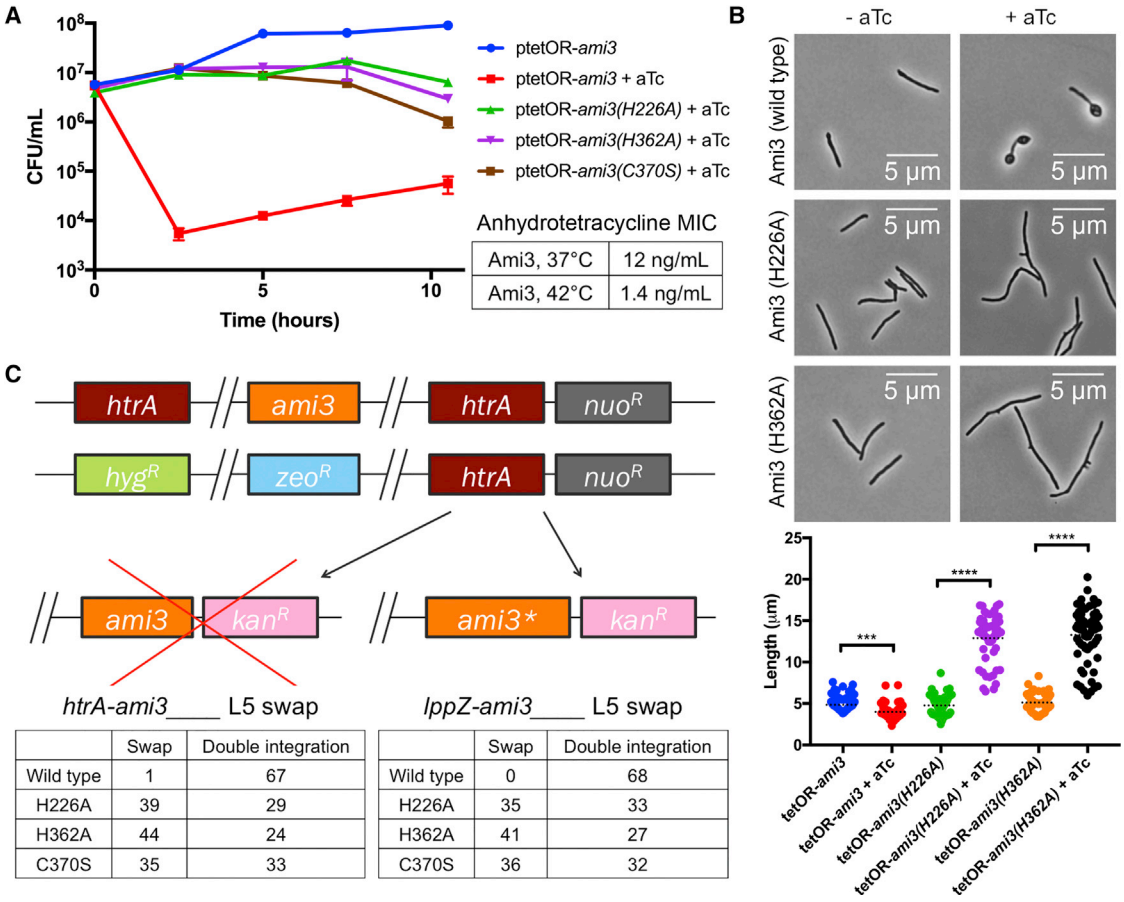

	Swap	Double integration
Wild type	1	67
H226A	39	29
H362A	44	24
C370S	35	33

	Swap	Double integration
Wild type	0	68
H226A	35	33
H362A	41	27
C370S	36	32

Figure 3. Ami3 Hyperactivity Is Toxic

(A) Overexpression of Ami3 is lethal. Left: strains expressing wild-type *ami3* or its catalytic mutants regulated by an aTc-inducible promoter were grown in the presence or absence of 100 ng/mL aTc (see Figure S3). Aliquots were taken at the indicated time points and analyzed for colony-forming units (CFUs). The uninduced wild-type *ami3* strain is representative of all uninduced strains. Error bars represent SD of the mean. Right: aTc MIC of wild-type *ami3* overexpression at different temperatures.

(B) Overexpression of different variants of Ami3 yields divergent phenotypes. Strains expressing wild-type *ami3* or its catalytic mutants regulated by an aTc-inducible promoter were grown in the presence or absence of 100 ng/mL aTc and observed under the microscope. At least 50 cells were quantified in each condition. Dotted black lines indicate data median. ***$p < 0.001$ and ****$p < 0.0001$.

(C) Ablation of Ami3 catalytic activity suppresses the essentiality of *htrA* and *lppZ*. Top: the endogenous copies of *ami3* and *htrA* were replaced with zeocin and hygromycin resistance cassettes, respectively, and a copy of *htrA* was integrated at the L5 phage integration site. *ami3* or a catalytically inactive variant of *ami3* (*ami3[H226A]*, *ami3[H362A]*, and *ami3[C370S]*), was transformed into this background. *ami3** indicates the respective *ami3* allele. Full swaps that acquire kanamycin resistance at the expense of nourseothricin resistance render strains devoid of *htrA* (or *lppZ*) and must thus carry a suppressor mutation. Bottom: quantification of *ami3* and *ami3** swaps. A total of 68 transformants were tested for antibiotic resistance. An equivalent swap was performed for *lppZ* and enumerated in the same manner.

by HtrA(S354A) induction; this is not due to a difference in stability between wild-type and catalytically inactive HtrA (Figure 1E). Increasing HtrA(S354A) expression further decreased Ami3 levels, but not to the levels achieved by wild-type HtrA (Figure 4B). Accordingly, strains expressing only HtrA(S354A) were more sensitive to Ami3 overexpression (Figure S3D). A similar but milder decrease in Ami3 protein levels was observed upon LppZ induction (Figure 4A), indicating that LppZ makes a less substantial contribution to Ami3 regulation.

Finally, we tested the dependency of the HtrA-LppZ interaction on the presence of its potential substrate Ami3. We found that HtrA and LppZ interacted even in a Δ*ami3* background (Figure S1D). We conclude that the HtrA-LppZ complex negatively regulates Ami3, with HtrA likely serving as the limiting factor and catalytic agent.

Pmt Stabilizes Ami3 through Mannosylation

Because loss of *pmt* suppressed the essentiality of *htrA* and *lppZ* (Figures 2B and 2D), we hypothesized that it might be a positive regulator of Ami3 toxicity by driving its accumulation. Pmt has been previously characterized as a periplasmic mannosyltransferase with a catalytic aspartic acid at residue 68 (D68) (VanderVen et al., 2005; Liu et al., 2013); however, few of its targets have been identified. We tested the importance of this activity by mutating the catalytic aspartic acid D68 to an alanine, which decreases mannosyltransferase activity by more than 50%

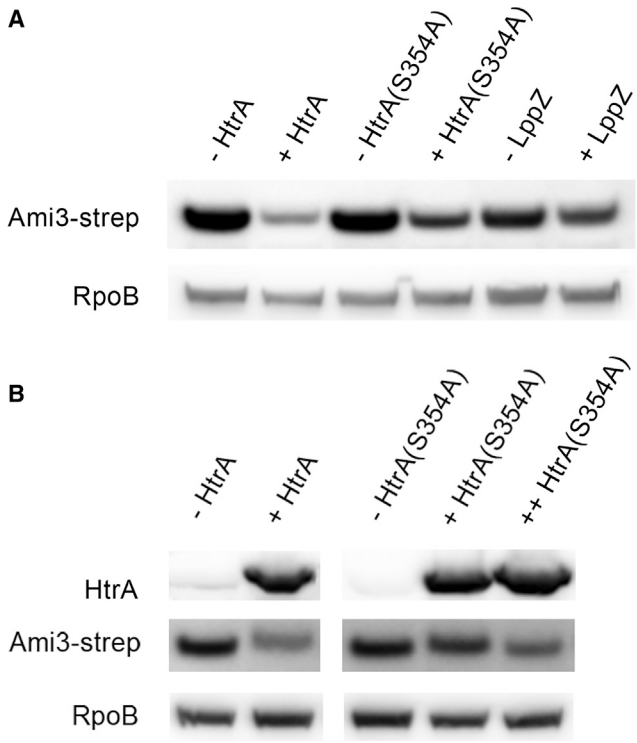

Figure 4. Induction of HtrA-LppZ Decreases Cellular Ami3 Levels

(A) HtrA and LppZ expression decrease Ami3 levels to varying degrees. Strains in which the only copy of *htrA* or *lppZ* was under an aTc-inducible promoter were constructed and grown with or without 100 ng/mL aTc for 12 hr. HtrA(S354A) is an allele of *htrA* presumed to exhibit reduced catalytic activity in HtrA homologs due to a mutation in its catalytic serine (see Figure S3). Whole-cell lysate was analyzed using western blotting using anti-Strep and anti-RpoB as a loading control.

(B) Higher expression of HtrA(S354A) further decreases Ami3. A second copy of aTc-inducible *htrA(S354A)* was transformed into the mutant strain described in (A), and all strains were grown with or without 100 ng/mL aTc for 8 hr. Whole-cell lysate was analyzed using western blotting using anti-Strep and anti-HtrA and anti-RpoB as a loading control. Western blot images were cropped but display all relevant lanes and reactive bands.

(VanderVen et al., 2005). Using an L5 swap, we found that *pmt(D68A)*, but not wild-type *pmt*, permitted growth of a strain missing either *htrA* or *lppZ* (Figure 5A).

To test if Ami3 is itself mannosylated by Pmt, we immunoprecipitated epitope-tagged Ami3, analyzed it using mass spectrometry, and found hexose modifications on three threonines: T122, T130, and T138 (Figures S4A and S4B; Table S1). These modifications were no longer detected when an Ami3 sample was isolated from a Δ*pmt* strain (Figure S4A; Table S1). Given that diverse hexose modifications emerge at similar molecular weights by mass spectrometry, we were not able to chemically confirm mannosylation; however, given our genetic data, we proceeded under the assumption that we had found a putative mannosylation. An allele substituting alanines for these residues (Ami3[T122A/T130A/T138A] or Ami3***) allowed growth of a strain lacking *htrA* (Figure 5B). We assessed the contribution of each mannosylated residue to Ami3 toxicity and found that T122 and T130 were critical, while T138 did not affect Ami3 toxicity (Figure S4C). To test whether mannosylation contributed to Ami3 stability, we monitored Ami3 levels by western blot in a Δ*pmt* strain (Figure 5C, left). Adding wild-type *pmt*, but not *pmt*(D68A), restored wild-type levels of Ami3. In contrast, Ami3*** was insensitive to the presence of Pmt (Figure 5C, right).

The simplest explanation for the effect of mannosylation on protein quantity is that modification affects protein stability. To test this, we assayed the half-life of Ami3 in wild-type and Δ*pmt* strains after inhibiting translation with chloramphenicol. Ami3 levels decreased significantly faster in the Δ*pmt* strain compared with wild-type cells (Figures 5D and 5E) demonstrating that mannosylation stabilizes Ami3.

Because Pmt increases Ami3 stability, we reasoned that overexpression of Ami3 in cells lacking *pmt* may be less toxic. Indeed, Ami3 overexpression in a Δ*pmt* background and Ami3*** overexpression exhibit less severe morphological defects and 5-fold increased survival compared with wild-type Ami3 overexpression (Figures 6A–6C and S5) To determine whether abundance and catalytic activity make independent contributions to toxicity, we monitored the growth of strains overexpressing Ami3(H362A), the catalytic mutant of Ami3 with protein levels most closely mimicking those of wild-type Ami3 (Figure S3B) in the Δ*pmt* background. As expected, growth of a strain overexpressing Ami3(H362A) was further rescued (Figure 6C) and its morphological defects were lessened (Figures 6A and 6B) by knocking out *pmt*. These results are consistent with a model in which Ami3 activity and stability are independent, and altering both in combination has an additive effect on relieving the toxicity of overexpression.

Finally, mannosylation does not appear to affect the interaction of HtrA and LppZ (Figure S1D). Additionally, HtrA still reduces Ami3 levels in a Δ*pmt* strain (Figure S4D), demonstrating that mannosylation is not required to elicit the activity of HtrA-LppZ against Ami3.

Amidases Have Redundant Functions in *Msm*

Although Ami3 has the potential to accumulate to toxicity, it is not an essential gene, and loss of *ami3* is not associated with any obvious phenotype (Figures S6A and S6B). However, Ami3 is not the only putative N-acetylmuramoyl-L-alanine amidase in *Msm*; Ami1 and Ami4 are also members of this family (Machowski et al., 2014), and several studies have presented evidence of Ami1's influence on normal cell division (Senzani et al., 2017; Li et al., 2018). In *E. coli*, amidases have redundant functions and are not individually essential for growth, and mutants missing multiple amidases remain viable (Heidrich et al., 2001; van Heijenoort, 2011). To test for similar redundancy in *Msm*, we constructed strains lacking individual and multiple amidases. We found that all of these strains had normal growth kinetics and morphologies (Figures S6A and S6B) but were altered in their accumulation of the fluorescent molecule calcein (Figure S6C). In accordance with previous studies (Rego et al., 2017), we found rifampin susceptibility in these mutants in a manner that correlated with calcein permeability (Figure S6D). However, loss of either *ami1* or *ami4* was unable to suppress *htrA* essentiality (Figure S6E), highlighting Ami3's unique contribution to necessitating the activity of HtrA-LppZ.

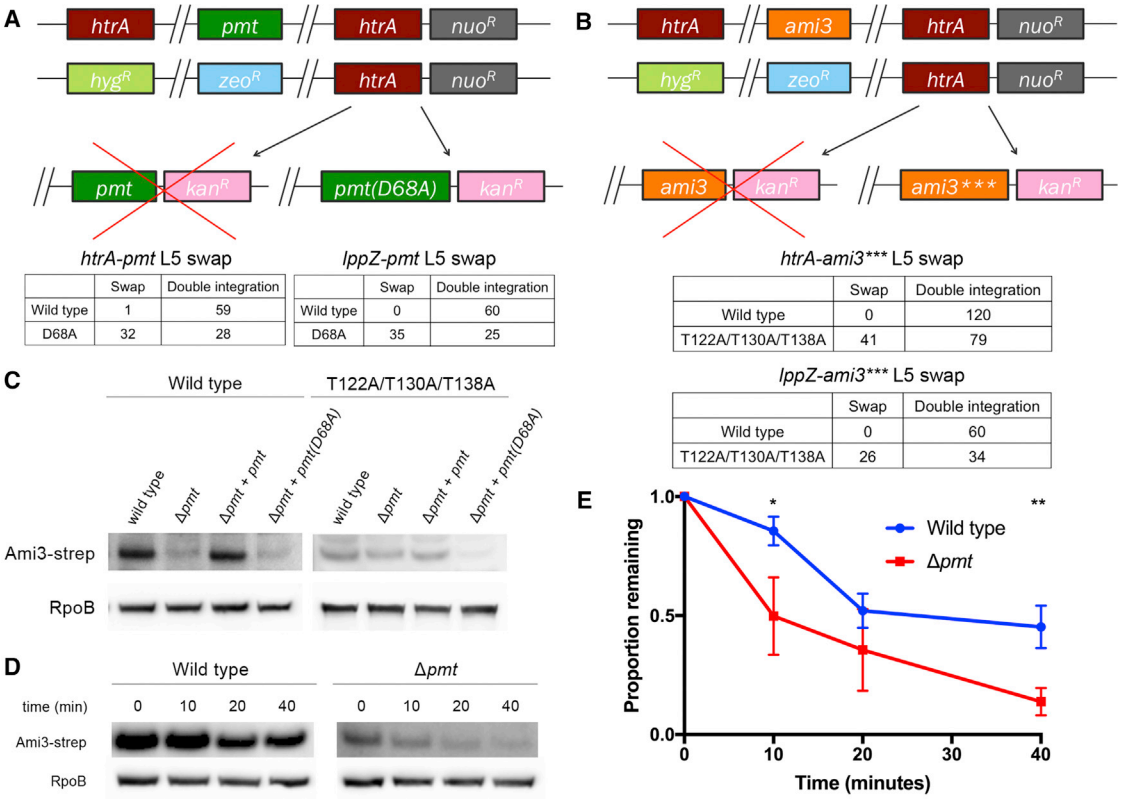

Figure 5. Pmt Mannosylation Stabilizes Ami3

(A) Mutating the catalytic activity of Pmt suppresses the essentiality of *htrA* and *lppZ*. Top: the endogenous copies of *pmt* and *htrA* were replaced with zeocin and hygromycin resistance cassettes, respectively, and a copy of *htrA* was integrated at the L5 phage integration site. *pmt* or *pmt(D68A)*, a catalytically inactive variant of *pmt*, was transformed into this background. Full swaps that acquire kanamycin resistance at the expense of nourseothricin resistance render strains devoid of *htrA* (or *lppZ*) and must thus carry a suppressor mutation. Bottom: quantification of *pmt* and *pmt(D68A)* swaps. A total of 60 transformants were tested for antibiotic resistance. An equivalent swap was performed for *lppZ* and enumerated in the same manner.

(B) Removing the mannosylation residues of Ami3 suppresses the essentiality of *htrA* and *lppZ*. Top: the endogenous copies of *ami3* and *htrA* were replaced with zeocin and hygromycin resistance cassettes, respectively, and a copy of *htrA* was integrated at the L5 phage integration site. *ami3* or *ami3(T122A/T130A/T138A)* (*ami3****), an allele of *ami3* in which all mannosylation sites have been mutated (see Figure S4), was transformed into this background. Full swaps that acquire kanamycin resistance at the expense of nourseothricin resistance render strains devoid of *htrA* (or *lppZ*) and must thus carry a suppressor mutation. Bottom: quantification of *ami3* and *ami3**** swaps. A total of 120 transformants were tested for antibiotic resistance. An equivalent swap was performed for *lppZ* and enumerated in the same manner; a total of 60 transformants were tested for antibiotic resistance.

(C) Ami3 levels decrease in cells missing Pmt. Strains expressing Ami3-Strep or Ami3*** in a wild-type, Δ*pmt*, Δ*pmt*+*pmt*, or Δ*pmt*+*pmt(D68A)* background were grown to log phase. Whole-cell lysate was analyzed using western blotting using anti-Strep and anti-RpoB as a loading control.

(D) Pmt mannosylation increases the stability of Ami3 protein. At indicated time points after adding chloramphenicol, aliquots of cells were lysed, and levels of Ami3-Strep were monitored using western blot. Results are representative of three independent experiments.

(E) Quantification of Ami3 stability. Independent values of RpoB-normalized levels of Ami3 from (D) quantified using densitometry analysis. Western blot images were cropped but display all relevant lanes and reactive bands. *$p < 0.05$ and **$p < 0.01$. Error bars represent SD of the mean.

DISCUSSION

Peptidoglycan hydrolases must be carefully regulated in a spatiotemporal manner to coordinate the complex processes of cell expansion and division. Dysregulation of cell wall enzymes has been shown to be toxic in species from *E. coli* to the various mycobacteria (van Heijenoort, 2011; Chao et al., 2013). The rapid turnover of cell wall requires an equally fast disposal of unwanted enzymes, and in the extracellular compartment, fewer mechanisms are available than in the cytoplasm. Proteolysis is one of the more rapid ways to effect change in the periplasm (Mukherjee et al., 2009; Festa et al., 2010). Protein processing and degradation have already been shown to play important roles in the fine-tuning of cell division proteins. For instance, the hydrolase RipA must be cleaved by the serine protease MarP to process peptidoglycan (Botella et al., 2017). Cleavage can also efficiently halt the activity of enzymes: PBPB is cleaved by the metalloprotease Rv2869 in *Mtb* during oxidative stress (Mukherjee et al., 2009). Finally, several factors involved in cell wall assembly have been shown to be targeted for pupylation and subsequent proteasomal degradation, including MurA, KasB, and MtrA (Festa et al., 2010). However, none of these proteolytic or processing systems are essential for viability and only take on critical roles under environmental stress.

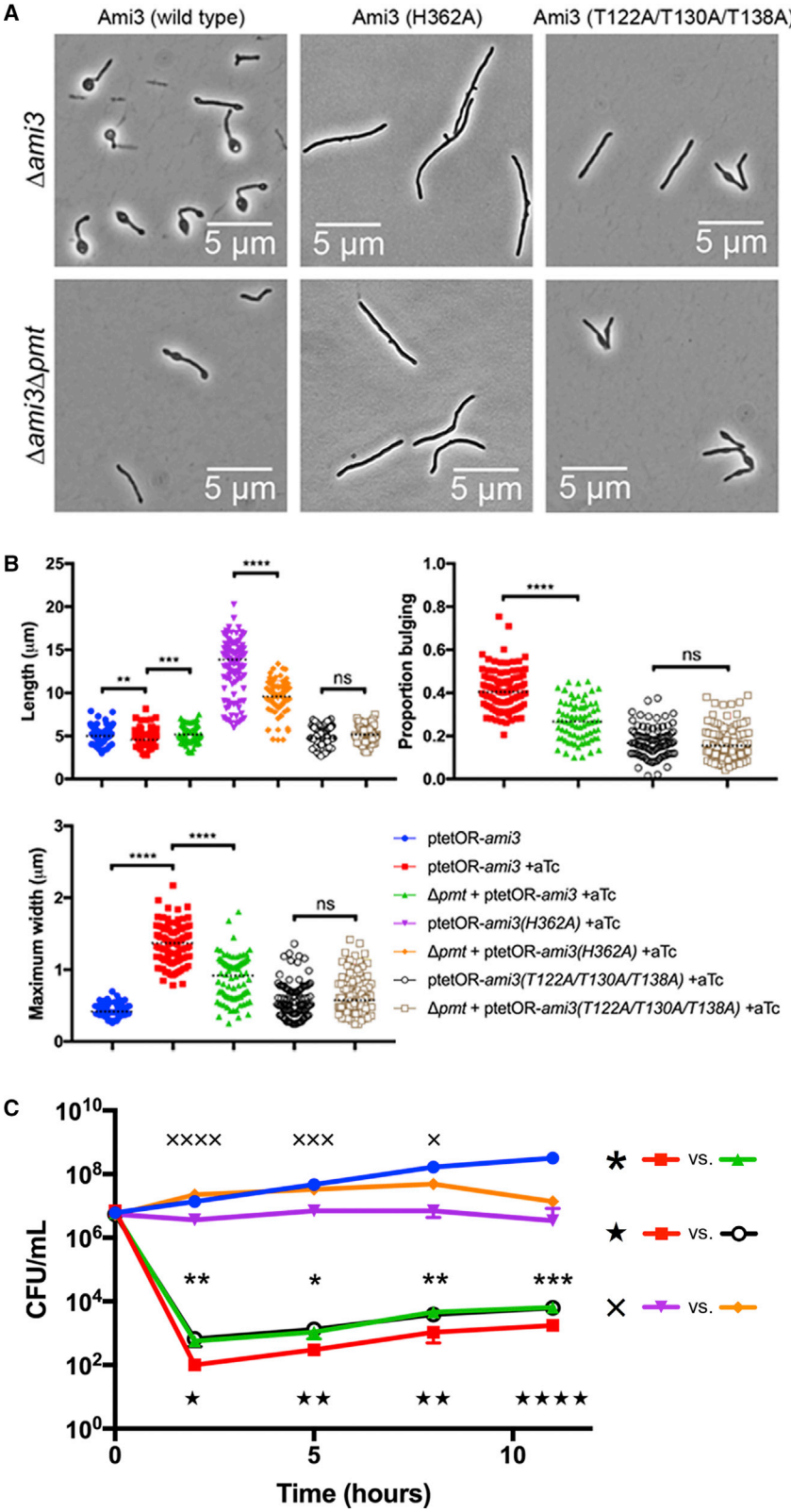

Figure 6. Removal of Mannosylation Partially Rescues Morphology and Survival of Ami3 Overexpression

(A) Loss of *pmt* relieves morphological defects in Ami3 overexpression. Wild-type *ami3*, *ami3(H362A)*, or *ami3**** was overexpressed in either Δ*ami3* or Δ*ami3*Δ*pmt* cells (see Figure S5).

(B) Quantification of cellular morphology of Ami3 overexpression. Cells were observed by microscopy and measured for total cell length, maximum cell width, and the proportion of the cell bulging (length of bulge over total cell length). At least 80 cells were quantified in each condition. Dotted black lines indicate median values.

(C) Survival and morphological quantification of Ami3 overexpression. Strains expressing wild-type *ami3*, *ami3(H362A)*, or *ami3**** under an aTc-inducible promoter were grown in the presence of absence or 100 ng/mL aTc. Aliquots were taken at the indicated time points for CFU analysis. The uninduced wild-type Ami3 strain is representative of all uninduced strains. The growth of various strains was compared, and demarcated by asterisks (comparing the overexpression of *ami3* in a wild-type or Δ*pmt* background), stars (comparing the overexpression of wild-type *ami3* or *ami3****), or X's (comparing the overexpression of *ami3(H362A)* in a wild-type or Δ*pmt* background).

*p < 0.05, **p < 0.01, ***p < 0.001, and ****p < 0.0001. Error bars represent SD of the mean.

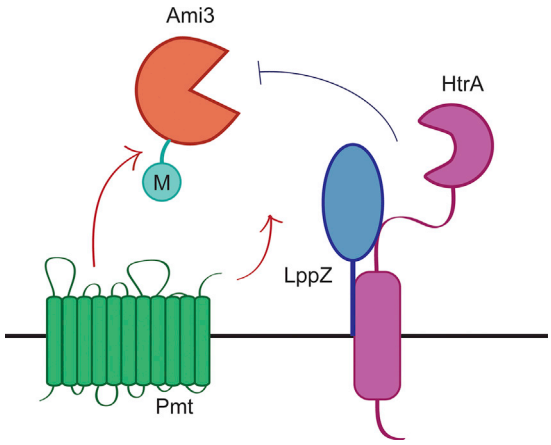

Figure 7. Model of HtrA-LppZ-Mediated Regulation of Ami3
The muramidase Ami3, under the stabilizing influence of Pmt, potentially accumulates to toxic levels over the course of the cell cycle. The HtrA-LppZ complex restores normal Ami3 levels to abrogate this lethality and is thus essential for viability.

We propose a model in which HtrA and LppZ are essential to degrade Ami3, thereby controlling its toxicity in *Msm* (Figure 7). Over the course of the cell cycle, preexisting cell wall material must be cleaved to make room for newly synthesized precursors. Cell wall hydrolases such as Ami3 are double-edged swords: although they are important for proper growth and septation, overactivity can destabilize the cell wall and lead to autolysis. Without spatiotemporal regulation, sustainable cellular growth cannot occur, thus necessitating the activity of a periplasmic protease such as HtrA that can regulate a highly active enzyme like Ami3 in *Msm*.

Notably, because Ami3 is still not completely stable even upon *htrA* depletion (Figures 5D and 5E), other proteases may have a more minor effect on Ami3 levels and will be the subject of future work.

The finding that HtrA requires a second protein is consistent with other observations of periplasmic proteases that rely on partners for fine-tuned regulation. Lipoproteins have been shown to be allosteric modulators of proteases in a variety of contexts (Tadokoro et al., 2004; Singh et al., 2015; Park et al., 2017) and have also been shown to directly activate the activity of cell wall enzymes (Paradis-Bleau et al., 2010; Typas et al., 2010; Egan et al., 2014; Lupoli et al., 2014). It is possible that LppZ facilitates the interaction between HtrA and Ami3, enhances the activity of HtrA, primes Ami3 for regulation by HtrA, or some combination of the above.

Although we were unable to measure amidase activity directly, Ami3 is likely a bona fide amidase on the basis of the phenotype of overexpression and requirement of catalytic residues for full toxicity, which mirror prior work in this field (Heidrich et al., 2001; Chao et al., 2013). In our work, all three N-acetylmuramoyl-L-alanine amidases in *Msm* are largely dispensable, though the importance of different amidases may vary in different *Msm* strains (Bavesh Kana, personal communication). Several alternative enzymes able to cleave peptidoglycan crosslinks likely operate in our strain under the growth conditions that we assayed, compensating for the loss of this family of amidases. Moreover, we simply may not know the growth condition in which these amidases play a critical role.

If Ami3 is indeed an active amidase, it is perhaps surprising that even a catalytically inactive variant of Ami3 can arrest cell growth. There are multiple possibilities to explain our observations. First, these mutants might retain a small amount of activity that stunts growth when enough protein is produced. Second, amidase activity may account for only a portion of *ami3* toxicity, which can still impair growth when expressed at high levels, perhaps by aggregating to levels the cell cannot tolerate. Third, Ami3 may engage with another cell wall enzyme that depends on Ami3 catalytic activity to execute its function. Enzymatically inactive Ami3 may thus lock its binding partner in a futile interaction that results in a failure to divide when the complex is sequestered or it fails to dissociate from peptidoglycan (Figure 3B). These models are not mutually exclusive.

In this context, mannosylation could alter protein folding or recognition by proteolytic enzymes. Post-translational modifications play an important role in the activation or stabilization of cell wall enzymes in mycobacteria. For instance, the peptidoglycan synthase PonA1 and MurA regulator CwlM must be phosphorylated to be active (Kieser et al., 2015; Boutte et al., 2016). Although this could also be a possible consequence of Ami3 mannosylation, it is unlikely given that *ami3* overexpression in a Δ*pmt* background does not phenocopy overexpression of catalytically inactive *ami3*. Additionally, *pmt* mannosylation does not appear to affect localization, as Ami3-mRFP is recruited to the same locales regardless of background (Figure S3B).

Furthermore, Pmt might play a broad role in cell wall maintenance, as it contributes to the virulence, immunogenicity, permeability, and antibiotic susceptibility of *Mtb* and *M. abscessus* (Becker et al., 2017; Liu et al., 2013; Deng et al., 2016; Harriff et al., 2017). In fact, a Δ*pmt* mutant in *M. abscessus* is more susceptible to several antibiotics including rifampin (Becker et al., 2017).

Proteases are attractive drug candidates, and in fact, an inhibitor of mycobacterial MarP and HtrA has been described (Zhao et al., 2015). However, at least for *Msm*, our results suggest that blocking HtrA could lead to high rates of resistance, as there are multiple mechanisms to escape drug-mediated killing. This might be less true for *Mtb*, especially during infection, when it is possible that Ami3 plays a larger role to maintain cellular integrity or HtrA, LppZ, and Pmt contribute to the pathogen's virulence in additional ways (Liu et al., 2013; Deng et al., 2016; Harriff et al., 2017). Notably, because *Mtb* and *Msm* differ in many ways, including the existence of a third *htrA* homolog, *pepA*, in *Mtb* only, our findings may not be entirely generalizable. However, given the retention of all three HtrA family proteins in multiple pathogenic mycobacteria (Lew et al., 2011), it is likely that these proteases serve critical roles worthwhile of future study. In this light, targeting of the essential HtrA-LppZ pathway remains possible.

STAR★METHODS

Detailed methods are provided in the online version of this paper and include the following:

SUPPLEMENTAL INFORMATION

Supplemental Information can be found online at https://doi.org/10.1016/j.celrep.2018.12.063.

ACKNOWLEDGMENTS

We thank the Taplin Mass Spectrometry facility at Harvard Medical School for help with mass spectrometry and the Microscopy Resources on the North Quad (MicRoN) core at Harvard Medical School for the use of microscopes and assistance with imaging. Additionally, we thank Sabine Ehrt and Helene Botella for the generous gift of the HtrA antibody. This research was supported by NIH grant F31 AI131502-01 and NSF graduate fellowship to K.J.W. and NIH grant U19 AI107774 to E.J.R. and T.R.I. These funding bodies had no part in the design of the study or collection, analysis, and interpretation of data or in writing the manuscript. Finally, we thank Thomas Bernhardt, Michael Chase, Simon Dove, Sarah Fortune, Darren Higgins, Marcia Goldberg, Christopher Sassetti, Lok To Sham, Matthew Waldor, and Junhao Zhu for helpful discussions.

AUTHOR CONTRIBUTIONS

K.J.W. and E.J.R. designed experiments and wrote the paper. K.J.W., C.C.B., and T.R.I. performed experiments and analyzed data.

DECLARATION OF INTERESTS

The authors declare no competing interests.

Received: May 2, 2018
Revised: October 14, 2018
Accepted: December 13, 2018
Published: May 21, 2019

REFERENCES

Becker, K., Haldimann, K., Selchow, P., Reinau, L.M., Dal Molin, M., and Sander, P. (2017). Lipoprotein glycosylation by protein-*O*-mannosyltransferase (MAB_1122c) contributes to low cell envelope permeability and antibiotic resistance of *Mycobacterium abscessus*. Front. Microbiol. *8*, 2123.

Botella, H., Vaubourgeix, J., Lee, M.H., Song, N., Xu, W., Makinoshima, H., Glickman, M.S., and Ehrt, S. (2017). *Mycobacterium tuberculosis* protease MarP activates a peptidoglycan hydrolase during acid stress. EMBO J. *36*, 536–548.

Boutte, C.C., Baer, C.E., Papavinasasundaram, K., Liu, W., Chase, M.R., Meniche, X., Fortune, S.M., Sassetti, C.M., Ioerger, T.R., and Rubin, E.J. (2016). A cytoplasmic peptidoglycan amidase homologue controls mycobacterial cell wall synthesis. Elife *5*, e14590.

Chao, M.C., Kieser, K.J., Minami, S., Mavrici, D., Aldridge, B.B., Fortune, S.M., Alber, T., and Rubin, E.J. (2013). Protein complexes and proteolytic activation of the cell wall hydrolase RipA regulate septal resolution in mycobacteria. PLoS Pathog. *9*, e1003197.

Clausen, T., Southan, C., and Ehrmann, M. (2002). The HtrA family of proteases: implications for protein composition and cell fate. Mol. Cell *10*, 443–455.

Clausen, T., Kaiser, M., Huber, R., and Ehrmann, M. (2011). HTRA proteases: regulated proteolysis in protein quality control. Nat. Rev. Mol. Cell Biol. *12*, 152–162.

DeJesus, M.A., and Ioerger, T.R. (2013). A hidden Markov model for identifying essential and growth-defect regions in bacterial genomes from transposon insertion sequencing data. BMC Bioinformatics *14*, 303–314.

Deng, G., Zhang, F., Yang, S., Kang, J., Sha, S., and Ma, Y. (2016). Mycobacterium tuberculosis Rv0431 expressed in Mycobacterium smegmatis, a potentially mannosylated protein, mediated the immune evasion of RAW 264.7 macrophages. Microb. Pathog. *100*, 285–292.

Egan, A.J., Jean, N.L., Koumoutsi, A., Bougault, C.M., Biboy, J., Sassine, J., Solovyova, A.S., Breukink, E., Typas, A., Vollmer, W., and Simorre, J.P. (2014). Outer-membrane lipoprotein LpoB spans the periplasm to stimulate the peptidoglycan synthase PBP1B. Proc. Natl. Acad. Sci. U S A *111*, 8197–8202.

Eng, J.K., McCormack, A.L., and Yates, J.R. (1994). An approach to correlate tandem mass spectral data of peptides with amino acid sequences in a protein database. J. Am. Soc. Mass Spectrom. *5*, 976–989.

Festa, R.A., McAllister, F., Pearce, M.J., Mintseris, J., Burns, K.E., Gygi, S.P., and Darwin, K.H. (2010). Prokaryotic ubiquitin-like protein (Pup) proteome of Mycobacterium tuberculosis [corrected]. PLoS ONE *5*, e8589.

Griffin, J.E., Gawronski, J.D., Dejesus, M.A., Ioerger, T.R., Akerley, B.J., and Sassetti, C.M. (2011). High-resolution phenotypic profiling defines genes essential for mycobacterial growth and cholesterol catabolism. PLoS Pathog. *7*, e1002251.

Harriff, M.J., Wolfe, L.M., Swarbrick, G., Null, M., Cansler, M.E., Canfield, E.T., Vogt, T., Toren, K.G., Li, W., Jackson, M., et al. (2017). HLA-E Presents Glycopeptides from the Mycobacterium tuberculosis Protein MPT32 to Human $CD8^+$ T cells. Sci. Rep. *7*, 4622.

Hartmans, S., and De Bont, J.A.M. (1992). The genus Mycobacterium—Nonmedical. In The Prokaryotes, Second Edition, M. Dowrkin, S. Falkow, E. Rosenberg, K.-H. Schleifer, and E. Stackebrandt, eds. (Springer-Verlag), pp. 1214–1237.

He, H., Hovey, R., Kane, J., Singh, V., and Zahrt, T.C. (2006). MprAB is a stress-responsive two-component system that directly regulates expression of sigma factors SigB and SigE in Mycobacterium tuberculosis. J. Bacteriol. *188*, 2134–2143.

Heidrich, C., Templin, M.F., Ursinus, A., Merdanovic, M., Berger, J., Schwarz, H., de Pedro, M.A., and Höltje, J.V. (2001). Involvement of N-acetylmuramyl-L-alanine amidases in cell separation and antibiotic-induced autolysis of Escherichia coli. Mol. Microbiol. *41*, 167–178.

Ingmer, H., and Brøndsted, L. (2009). Proteases in bacterial pathogenesis. Res. Microbiol. *160*, 704–710.

Kapopoulou, A., Lew, J.M., and Cole, S.T. (2011). The MycoBrowser portal: a comprehensive and manually annotated resource for mycobacterial genomes. Tuberculosis (Edinb). *91*, 8–13.

Kelley, L.A., Mezulis, S., Yates, C.M., Wass, M.N., and Sternberg, M.J. (2015). The Phyre2 web portal for protein modeling, prediction and analysis. Nat. Protoc. *10*, 845–858.

Kieser, K.J., Boutte, C.C., Kester, J.C., Baer, C.E., Barczak, A.K., Meniche, X., Chao, M.C., Rego, E.H., Sassetti, C.M., Fortune, S.M., and Rubin, E.J. (2015). Phosphorylation of the Peptidoglycan Synthase PonA1 Governs the Rate of Polar Elongation in Mycobacteria. PLoS Pathog. *11*, e1005010.

Lew, J.M., Kapopoulou, A., Jones, L.M., and Cole, S.T. (2011). TubercuList—10 years after. Tuberculosis (Edinb). *91*, 1–7.

Lewis, J.A., and Hatfull, G.F. (2003). Control of directionality in L5 integrase-mediated site-specific recombination. J. Mol. Biol. *326*, 805–821.

Li, X., He, J., Fu, W., Cao, P., Zhang, S., and Jiang, T. (2018). Effect of Mycobacterium tuberculosis Rv3717 on cell division and cell adhesion. Microb. Pathog. *117*, 184–190.

Liu, C.F., Tonini, L., Malaga, W., Beau, M., Stella, A., Bouyssié, D., Jackson, M.C., Nigou, J., Puzo, G., Guilhot, C., et al. (2013). Bacterial protein-O-mannosylating enzyme is crucial for virulence of Mycobacterium tuberculosis. Proc. Natl. Acad. Sci. U S A *110*, 6560–6565.

Lupoli, T.J., Lebar, M.D., Markovski, M., Bernhardt, T., Kahne, D., and Walker, S. (2014). Lipoprotein activators stimulate Escherichia coli penicillin-binding proteins by different mechanisms. J. Am. Chem. Soc. *136*, 52–55.

Machowski, E.E., Senzani, S., Ealand, C., and Kana, B.D. (2014). Comparative genomics for mycobacterial peptidoglycan remodelling enzymes reveals extensive genetic multiplicity. BMC Microbiol. *14*, 75.

Manganelli, R., Fattorini, L., Tan, D., Iona, E., Orefici, G., Altavilla, G., Cusatelli, P., and Smith, I. (2004). The extra cytoplasmic function sigma factor sigma(E) is essential for Mycobacterium tuberculosis virulence in mice. Infect. Immun. *72*, 3038–3041.

Mukherjee, P., Sureka, K., Datta, P., Hossain, T., Barik, S., Das, K.P., Kundu, M., and Basu, J. (2009). Novel role of Wag31 in protection of mycobacteria under oxidative stress. Mol. Microbiol. *73*, 103–119.

Paradis-Bleau, C., Markovski, M., Uehara, T., Lupoli, T.J., Walker, S., Kahne, D.E., and Bernhardt, T.G. (2010). Lipoprotein cofactors located in the outer membrane activate bacterial cell wall polymerases. Cell *143*, 1110–1120.

Park, H., Kim, Y.T., Choi, C., and Kim, S. (2017). Tripodal lipoprotein variants with C-terminal hydrophobic residues allosterically modulate activity of the DegP protease. J. Mol. Biol. *429*, 3090–3101.

Pashley, C.A., and Parish, T. (2003). Efficient switching of mycobacteriophage L5-based integrating plasmids in Mycobacterium tuberculosis. FEMS Microbiol. Lett. *229*, 211–215.

Peng, J., and Gygi, S.P. (2001). Proteomics: the move to mixtures. J. Mass Spectrom. *36*, 1083–1091.

Pham, T.T., Jacobs-Sera, D., Pedulla, M.L., Hendrix, R.W., and Hatfull, G.F. (2007). Comparative genomic analysis of mycobacteriophage Tweety: evolutionary insights and construction of compatible site-specific integration vectors for mycobacteria. Microbiology *153*, 2711–2723.

Raju, R.M., Goldberg, A.L., and Rubin, E.J. (2012a). Bacterial proteolytic complexes as therapeutic targets. Nat. Rev. Drug Discov. *11*, 777–789.

Raju, R.M., Unnikrishnan, M., Rubin, D.H., Krishnamoorthy, V., Kandror, O., Akopian, T.N., Goldberg, A.L., and Rubin, E.J. (2012b). Mycobacterium tuberculosis ClpP1 and ClpP2 function together in protein degradation and are required for viability in vitro and during infection. PLoS Pathog. *8*, e1002511.

Raju, R.M., Jedrychowski, M.P., Wei, J.R., Pinkham, J.T., Park, A.S., O'Brien, K., Rehren, G., Schnappinger, D., Gygi, S.P., and Rubin, E.J. (2014). Post-translational regulation via Clp protease is critical for survival of Mycobacterium tuberculosis. PLoS Pathog. *10*, e1003994.

Rego, E.H., Audette, R.E., and Rubin, E.J. (2017). Deletion of a mycobacterial divisome factor collapses single-cell phenotypic heterogeneity. Nature *546*, 153–157.

Schwechheimer, C., Rodriguez, D.L., and Kuehn, M.J. (2015). NlpI-mediated modulation of outer membrane vesicle production through peptidoglycan dynamics in Escherichia coli. MicrobiologyOpen *4*, 375–389.

Senzani, S., Li, D., Bhaskar, A., Ealand, C., Chang, J., Rimal, B., Liu, C., Joon Kim, S., Dhar, N., and Kana, B. (2017). An amidase_3 domain-containing N-acetylmuramyl-L-alanine amidase is required for mycobacterial cell division. Sci. Rep. *7*, 1140.

Shevchenko, A., Wilm, M., Vorm, O., and Mann, M. (1996). Mass spectrometric sequencing of proteins silver-stained polyacrylamide gels. Anal. Chem. *68*, 850–858.

Singh, S.K., Parveen, S., SaiSree, L., and Reddy, M. (2015). Regulated proteolysis of a cross-link-specific peptidoglycan hydrolase contributes to bacterial morphogenesis. Proc. Natl. Acad. Sci. U S A *112*, 10956–10961.

Tadokoro, A., Hayashi, H., Kishimoto, T., Makino, Y., Fujisaki, S., and Nishimura, Y. (2004). Interaction of the Escherichia coli lipoprotein NlpI with periplasmic Prc (Tsp) protease. J. Biochem. *135*, 185–191.

Typas, A., Banzhaf, M., van den Berg van Saparoea, B., Verheul, J., Biboy, J., Nichols, R.J., Zietek, M., Beilharz, K., Kannenberg, K., von Rechenberg, M., et al. (2010). Regulation of peptidoglycan synthesis by outer-membrane proteins. Cell *143*, 1097–1109.

van Heijenoort, J. (2011). Peptidoglycan hydrolases of Escherichia coli. Microbiol. Mol. Biol. Rev. *75*, 636–663.

van Kessel, J.C., and Hatfull, G.F. (2008). Mycobacterial recombineering. Methods Mol. Biol. *435*, 203–215.

VanderVen, B.C., Harder, J.D., Crick, D.C., and Belisle, J.T. (2005). Export-mediated assembly of mycobacterial glycoproteins parallels eukaryotic pathways. Science *309*, 941–943.

White, M.J., He, H., Penoske, R.M., Twining, S.S., and Zahrt, T.C. (2010). PepD participates in the mycobacterial stress response mediated through MprAB and SigE. J. Bacteriol. *192*, 1498–1510.

White, M.J., Savaryn, J.P., Bretl, D.J., He, H., Penoske, R.M., Terhune, S.S., and Zahrt, T.C. (2011). The HtrA-like serine protease PepD interacts with and modulates the Mycobacterium tuberculosis 35-kDa antigen outer envelope protein. PLoS ONE *6*, e18175.

World Health Organization (2017). Global Tuberculosis Report (Geneva: World Health Organization).

Zhang, Y.J., Ioerger, T.R., Huttenhower, C., Long, J.E., Sassetti, C.M., Sacchettini, J.C., and Rubin, E.J. (2012). Global assessment of genomic regions required for growth in Mycobacterium tuberculosis. PLoS Pathog. *8*, e1002946.

Zhao, N., Darby, C.M., Small, J., Bachovchin, D.A., Jiang, X., Burns-Huang, K.E., Botella, H., Ehrt, S., Boger, D.L., Anderson, E.D., et al. (2015). Target-based screen against a periplasmic serine protease that regulates intrabacterial pH homeostasis in Mycobacterium tuberculosis. ACS Chem. Biol. *10*, 364–371.

STAR★METHODS

KEY RESOURCES TABLE

REAGENT or RESOURCE	SOURCE	IDENTIFIER
Antibodies		
Rabbit polyclonal anti-Strep-tag II (NWSHPQFEK)	GenScript	Cat#89494-724
Rabbit polyclonal anti-FLAG	Sigma Aldrich	Cat#F7425
Rabbit polyclonal anti-HtrA	Helene Botella and Sabine Ehrt	N/A
Mouse polyclonal anti-RpoB	ThermoFisher Scientific	Cat#MA1-25425
Bacterial Strains		
Escherichia coli TOP10	ThermoFisher Scientific (formerly Invitrogen)	Cat#404010
Msm mc2 155	Laboratory of Barry Bloom	N/A
Full list of strains in Table S2	This paper	N/A
Chemicals, Peptides, and Recombinant Proteins		
MagStrep type3 XT Beads, 5% suspension	IBA Life Sciences	Cat#2-4090-002
Anti-FLAG M2 Magnetic Beads	Sigma Aldrich	Cat#M8823
FLAG peptide	Sigma Aldrich	Cat#F3290
Concanavalin A from *Canavalia ensiformis* (Jack bean) peroxidase conjugate	Sigma Aldrich	Cat#L6397
Pierce Avidin Agarose	ThermoFisher Scientific	Cat#20219
10X Buffer BXT	IBA Life Sciences	Cat#2-1042-025
Deposited Data		
Full, uncropped Western blots	This paper	https://doi.org/10.17632/r7mm9mtt3v.1#folder-26c6e562-7d8d-44c8-a65a-21fa0ae692eb
Oligonucleotides		
Full list of plasmids and strains in Table S2	This paper	N/A
Software and Algorithms		
ImageJ	National Institutes of Health	https://imagej.nih.gov/ij/download.html

CONTACT FOR REAGENT AND RESOURCE SHARING

Further information and requests for resources and reagents should be directed to and will be fulfilled by the Lead Contact, Eric J. Rubin (erubin@hsph.harvard.edu).

EXPERIMENTAL MODEL DETAILS

Msm mc^2155 was grown in liquid media containing 7H9 salts (Becton Dickinson) supplemented with 5 g/L albumin, 2 g/L dextrose, 0.85 g/L NaCl, 0.003 g/L catalase, 0.2% glycerol, and 0.05% Tween80, or plated on LB agar. For all oxidative stress experiments, strains were grown in Hartmans-de Bont (HdB) media, which was made as described (Hartmans and De Bont, 1992) with 0.05% Tween80. *E. coli* TOP10 was used for cloning. Antibiotic selection concentrations for *M. smegmatis* were as follows: 25 μg/mL kanamycin, 50 μg/mL hygromycin, 20 μg/mL zeocin, 20 μg/mL nourseothricin, and 5 μg/mL gentamicin. Antibiotic concentrations for *E. coli* were as follows: 50 μg/mL kanamycin, 100 μg/mL hygromycin, 50 μg/mL zeocin, and 40 μg/mL nourseothricin. Anhydrotetracyline was used at 100 ng/mL for gene induction or repression. All strains were grown at 37°C unless otherwise indicated.

METHOD DETAILS

Strain construction

Deletions of *htrA* and *lppZ* were generated by first transforming in a second copy of the gene at the L5 and Tweety phage integration sites (Lewis and Hatfull 2003; Pham et al. 2007), then using mycobacterial recombineering as previously described (van Kessel and Hatfull 2008) to delete the endogenous copy. Where indicated, *htrA* and *lppZ* were cloned into vectors with a tetON repressor to make their expression tetracycline inducible, or into vectors with a tetOFF repressor to make their expression tetracycline repressible.

All other deletions (*ami3, pmt,* and *mprB*) were generated by recombineering. To make the inducible overexpression strain, *ami3* was sub-cloned into a multi-copy episomal vector carrying both the tet operator and the tet repressor.

L5 swaps were performed as previously described (Pashley and Parish 2003); this technique was used to 1) test essentiality and suppression where indicated and/or 2) generate different allelic variants of *htrA* or *lppZ*. When testing essentiality or suppression, 60-200 colonies were patched for kanamycin and nourseothricin resistance.

A full list of strain details, including genotypes, plasmids, and primers, is available in Table S2.

Microscopy and image analysis

Still images were taken of cells immobilized on agar pads on a Nikon Ti inverted widefield epifluorescence microscope with a Photometrics coolSNAP CCD monochrome camera and a Plan Apo 100X objective with a numerical aperture of 1.4. Images were processed using NIS Elements version 4.3 and ImageJ. All aTc-repressible and -inducible strains were depleted or induced by the addition of 100 ng/mL anhydrotetracycline (aTc). The red fluorescent

405 images were taken with a 528-553 excitation filter and a 590-650 emission filter.

Growth rate determination and kill curves

For growth curves, strains were grown to mid-log phase, diluted to OD_{600} 0.005 in triplicate, and measured every 15 min in a Bioscreen growth curve machine (Growth Curves USA) at 37°C or 42°C, where indicated.

For environmental stress kill curves, strains were grown to mid-log phase, washed twice with PBS-Tween80, diluted to OD600 0.05, and rolled at 37°C in PBS-Tween80 or HdB + 0.02% tert-butyl hydroperoxide. At the indicated time points, 200 uL aliquots were removed, serially diluted in PBS-Tween80, and plated for CFUs.

For aTc-inducible overexpression kill curves, all steps were the same except cells were not washed before subculturing into 7H9 with kanamycin to maintain the episomal plasmid, with or without 100 ng/mL aTc.

Tert-butyl hydroperoxide and aTc were added once at the beginning of each experiment. Each kill curve was performed at least thrice, in triplicate, with similar results.

Immunoprecipitation and western blotting

To identify potential interactors of HtrA, 200 mL mid-log phase cultures of a strain expressing HtrA-Strep and an untagged control were spun down and resuspended in 2 mL of Buffer W (100 mM Tris, 150 mM NaCl, 1 mM EDTA) with an EDTA-free protease inhibitor cocktail (Roche, Switzerland). The cells were lysed by bead beating and SDS was added to the lysate to a final concentration of 1%. The lysate was pre-cleared of endogenously biotinylated proteins using Pierce Avidin Agarose for 1 hour at room temperature. The cleared supernatant was then added to MagStrep ''type3'' XT beads (IBA Lifesciences) and incubated overnight at 4°C. The beads were then washed three times with Buffer W and eluted using Buffer BXT (IBA Lifesciences). The eluted samples were separated on a 4%–12% NuPAGE Bis-Tris precast gel (Invitrogen Novex) and stained with Coomassie Blue. The entire lanes of eluted protein from the HtrA-Strep and untagged control immunoprecipitations were cut out and analyzed by the Harvard Taplin mass spectrometry facility. The unbiased immunoprecipitation was performed twice, both identifying LppZ as the top hit enriched in HtrA-Strep compared to the untagged control. To search for mannosylation residues in Ami3-Strep, all steps were performed as above except single bands were excised instead of entire lanes.

For co-immunoprecipitations, 100 mL cultures were split in two and all steps were performed as above for samples incubated with MagStrep beads. For immunoprecipitations using α-FLAG M2 Magnetic Beads (Sigma Aldrich), SDS was not added, pre-clearing with avidin agarose was skipped, and elution was carried out with FLAG peptide. Co-immunoprecipitations were analyzed by western blotting.

For western blots, cultures were spun down, resuspended in IP buffer (10 mM Tris-HCl (pH 8), 100 mM NaCl, 1 mM EDTA), and lysed by bead beating. Supernatants were normalized by A280 protein concentration, diluted with 6X Laemmli buffer, and run on SDS-PAGE gels with 4%–12% NuPAGE Bis Tris precast gels (Life Technologies). Membranes were blotted with rabbit α-FLAG (Sigma Aldrich) at 1:1000 in TBST + 5% milk, rabbit α-Strep (Genscript) at 1:1000 in TBST + 3% BSA, mouse α-RpoB (ThermoFisher Scientific) at 1:1000 in TBST + 5% milk, and rabbit α-HtrA (a generous gift from Helene Botella and Sabine Ehrt) at 1:1000 in TBST + 5% milk. For co-immunoprecipitation blots, the relevant fractions were run on a single membrane, blotted first with one antibody, stripped with Restore Western Blot Stripping Buffer (ThermoFisher Scientific 21059), and reblotted with the inverse.

MIC determination

The MIC of *M. smegmatis* strains were performed using the Alamar Blue assay as previously described (Kieser et al. 2015).

Calcein staining and flow cytometry

Mid-log-phase cultures were stained with 0.5 μg/mL calcein for 1 hour at 37°C. These cells were then analyzed by flow cytometry (MACSQuant VYB excitation: 488 nm; emission filter: 525/50).

Total cell length, bulge length, maximum cell width, and mean fluorescence intensity (MFI) were measured manually where indicated.

Hexose modification analysis by LC-MS/MS

To identify potential hexose modifications on Ami3, a 200 mL mid-log phase cultures of strains expressing Ami3-Strep in a wild-type or Δ*pmt* background were spun down and resuspended in 2 mL of Buffer W (100 mM Tris, 150 mM NaCl, 1 mM EDTA) with an EDTA-free protease inhibitor cocktail (Roche, Switzerland). The cells were lysed by bead beating and SDS was added to the lysate to a final concentration of 1%. The lysate was pre-cleared of endogenously biotinylated proteins using Pierce Avidin Agarose for 1 hour at room temperature. The cleared supernatant was then added to MagStrep "type3" XT beads (IBA Lifesciences) and incubated overnight at 4°C. The beads were then washed three times with Buffer W and eluted using Buffer BX (IBA Lifesciences). The eluted samples were separated on a 4%–12% NuPAGE Bis-Tris precast gel (Invitrogen Novex) and stained with Coomassie Blue. A single band running at the predicted molecular weight of Ami3-Strep was excised from each sample.

The samples were reduced with 1 mM DTT for 30 minutes at 60°C, then alkylated with 5mM iodoacetamide for 15 minutes at room temperature in the dark. Samples were then subjected to a modified in-gel trypsin digestion procedure (Shevchenko et al. 1996). Gel pieces were washed and dehydrated with acetonitrile for 10 minutes, followed by removal of acetonitrile and complete drying in a speed-vac. Rehydration of the gel pieces was performed with an 50 mM ammonium bicarbonate solution containing 12.5 ng/μl modified sequencing-grade trypsin (Promega, Madison, WI) at 4°C. Samples were then incubated at 37°C overnight. Peptides were later extracted by removing the ammonium bicarbonate solution, followed by one wash with a solution containing 50% acetonitrile and 1% formic acid. The extracts were then dried in a speed-vac for about an hour. The samples were then stored at 4°C until further analysis, upon which samples were reconstituted in 5 to 10 μl of HPLC solvent A (2.5% acetonitrile, 0.1% formic acid). A nano-scale reverse-phase HPLC capillary column was created by packing 2.6 μm C18 spherical silica beads into a fused silica capillary (100 μm inner diameter x ~30 cm length) with a flame-drawn tip (Peng and Gygi 2001). After the column was equilibrated, each sample was loaded onto the column via a Famos auto sampler (LC Packings, San Francisco, CA). A gradient was formed and peptides were eluted with increasing concentrations of solvent B (97.5% acetonitrile, 0.1% formic acid).

As each peptide was eluted, it was subjected to electrospray ionization and then entered into an LTQ Orbitrap Velos Pro ion-trap mass spectrometer (Thermo Fisher Scientific, San Jose, CA). Eluting peptides were detected, isolated, and fragmented to produce a tandem mass spectrum of specific fragment ions for each peptide. Peptide sequences were determined by matching the acquired fragmentation pattern with the Ami3 amino acid sequence, using a software program, Sequest (ThermoFinnigan, San Jose, CA) (Eng et al. 1994). The modification of 180.156 mass units to serine, and threonine was included in the database searches to determine hexose-modified peptides. Modifications were scored from 0 to 1000. Scores over 19 were considered confidently assigned. Scores of 1000 were considered unequivocal. All databases include a reversed version of all the sequences and the data was filtered to between a one and two percent peptide false discovery rate.

QUANTIFICATION AND STATISTICAL ANALYSIS

Statistical details of experiments can be found in the figure legends. All experiments were performed at least twice. Means were compared using a two-sided Student's t test, and all error bars indicate standard deviation around the mean. $p < 0.05$ was considered significant. For most microscopy experiments, roughly 100-200 cells were analyzed and data medians are shown. No statistical methods were used to predetermine sample size, and the researchers were not blinded to sample identity.

DATA AND SOFTWARE AVAILABILITY

Full, uncropped Western blots for relevant figures have been deposited to the Mendeley database under the following DOI: https://doi.org/10.17632/r7mm9mtt3v.1#folder-26c6e562-7d8d-44c8-a65a-21fa0ae692eb.

Cell Reports, Volume *27*

Supplemental Information

Mycobacterium smegmatis HtrA Blocks the Toxic Activity of a Putative Cell Wall Amidase

Katherine J. Wu, Cara C. Boutte, Thomas R. Ioerger, and Eric J. Rubin

SUPPLEMENTAL FIGURES

Figure S1

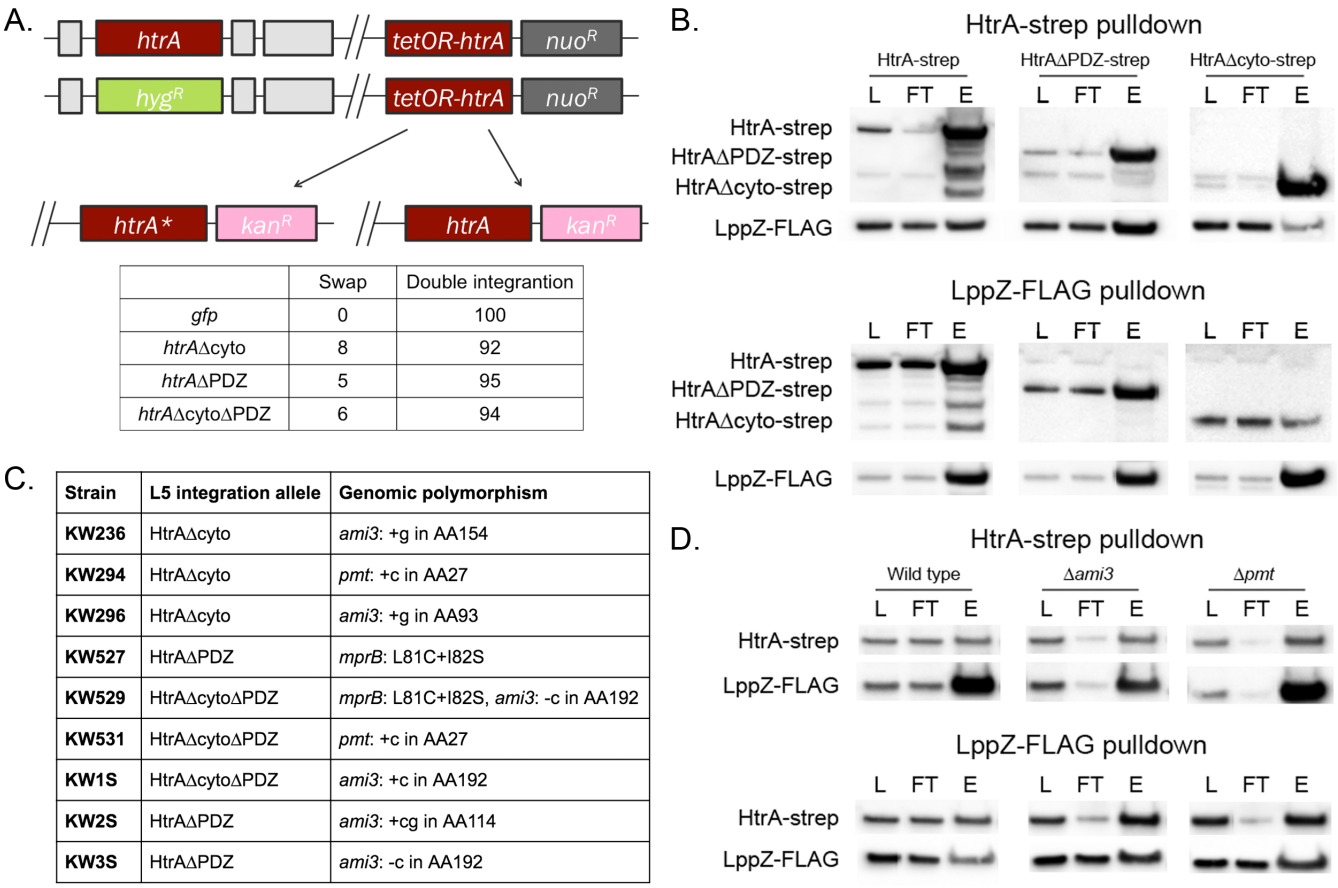

	Swap	Double integrantion
gfp	0	100
*htrA*Δcyto	8	92
*htrA*ΔPDZ	5	95
*htrA*ΔcytoΔPDZ	6	94

C.

Strain	L5 integration allele	Genomic polymorphism
KW236	HtrAΔcyto	*ami3*: +g in AA154
KW294	HtrAΔcyto	*pmt*: +c in AA27
KW296	HtrAΔcyto	*ami3*: +g in AA93
KW527	HtrAΔPDZ	*mprB*: L81C+I82S
KW529	HtrAΔcytoΔPDZ	*mprB*: L81C+I82S, *ami3*: -c in AA192
KW531	HtrAΔcytoΔPDZ	*pmt*: +c in AA27
KW1S	HtrAΔcytoΔPDZ	*ami3*: +c in AA192
KW2S	HtrAΔPDZ	*ami3*: +cg in AA114
KW3S	HtrAΔPDZ	*ami3*: -c in AA192

Figure S1, related to Figure 2: HtrA suppressor screen and HtrA-LppZ interactions. A. The cytoplasmic and PDZ domains of HtrA are essential for viability. Top: a schematic of the L5 essentiality swap. Placing a second copy of *htrA,* along with a nourseothricin resistance cassette, at the L5 phage integration site allows replacement of endogenous *htrA* with a hygromycin resistance cassette. The L5-integrated copy of *htrA* can be swapped for another copy of *htrA* attached to another antibiotic resistance marker, but not for truncations of *htrA* missing the cytoplasmic and/or PDZ domains (*htrA**). Bottom: quantification of *htrA* swaps. A total of 100 transformants were tested for antibiotic resistance. **B. HtrA and LppZ still interact even when the PDZ or cytoplasmic domains of HtrA are removed.** Different alleles of HtrA-Strep and LppZ-FLAG were individually immunoprecipitated using anti-Strep and anti-FLAG magnetic beads, respectively, and the following fractions were analyzed by Western blot: L = lysate, FT = flow through, E = elution. **C. Successful HtrA truncation swaps were whole genome sequenced for extragenic suppressors.** All strains sequenced carried mutations in *ami3, pmt*, and/or *mprB.* **D. HtrA and LppZ interact even in the absence of Ami3 or Pmt.** In the indicated genetic backgrounds, HtrA-Strep and LppZ-FLAG were individually immunoprecipitated using anti-Strep and anti-FLAG magnetic beads, respectively, and the

following fractions were analyzed by Western blot: L = lysate, FT = flow through, E = elution. Western blot images were cropped, but display all relevant lanes and reactive bands.

Figure S2

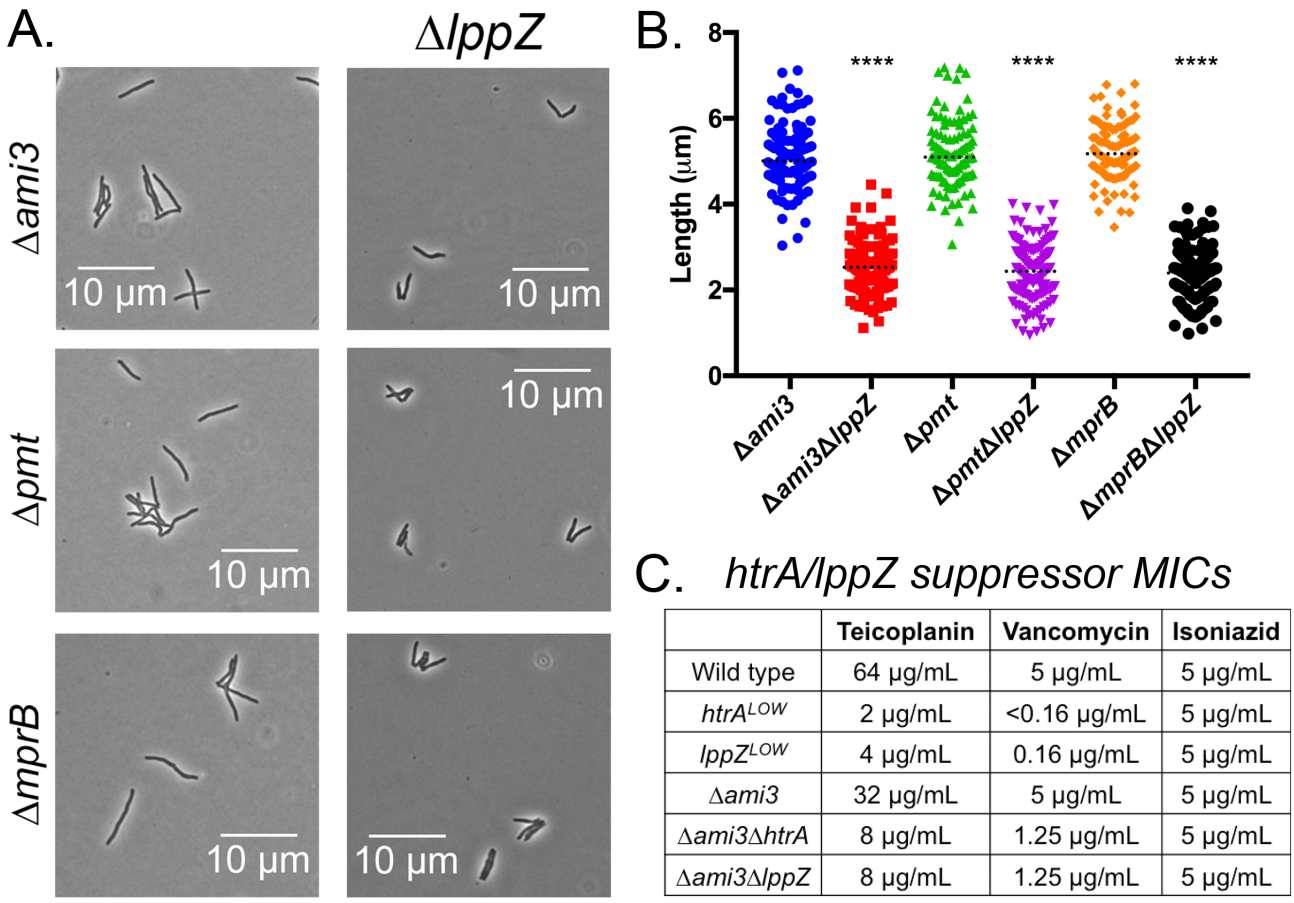

C. *htrA/lppZ suppressor MICs*

	Teicoplanin	Vancomycin	Isoniazid
Wild type	64 μg/mL	5 μg/mL	5 μg/mL
htrA^{LOW}	2 μg/mL	<0.16 μg/mL	5 μg/mL
lppZ^{LOW}	4 μg/mL	0.16 μg/mL	5 μg/mL
Δ*ami3*	32 μg/mL	5 μg/mL	5 μg/mL
Δ*ami3*Δ*htrA*	8 μg/mL	1.25 μg/mL	5 μg/mL
Δ*ami3*Δ*lppZ*	8 μg/mL	1.25 μg/mL	5 μg/mL

Figure S2, related to Figure 2: Suppressors of *htrA* essentiality also suppress *lppZ* essentiality and produce morphologically similar cells. A and B. Morphology of *lppZ* suppressor strains. Single suppressor knockouts and *lppZ* double knockouts were grown to log phase and analyzed for total cell length. At least 100 cells were quantified in each condition. Dotted black lines indicate median values. **** = p-value <0.0001. **C. Loss of *htrA* or *lppZ* in a suppressor background partially rescues antibiotic susceptibility.** The indicated strains were grown in teicoplanin, vancomycin, and isoniazid.

Figure S3

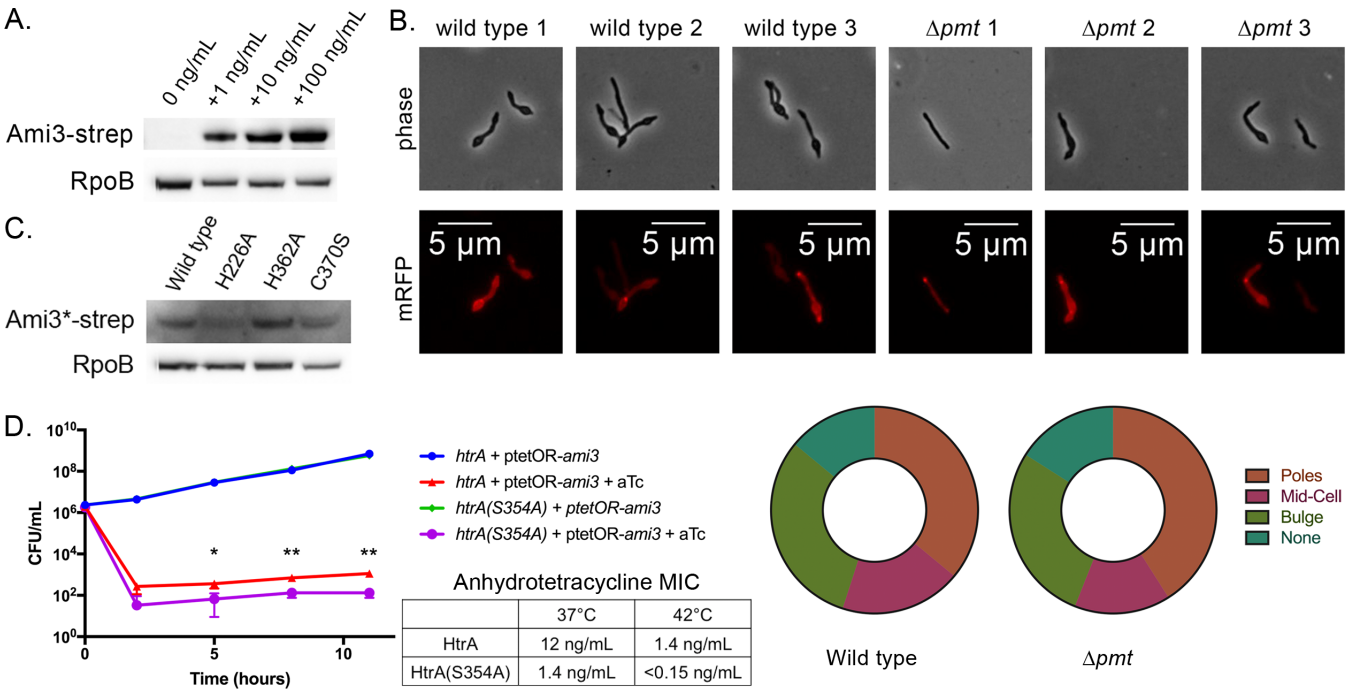

Figure S3, related to Figure 3 and Figure 4: Variable toxicity of Ami3. A. Different amounts of aTc induce different amounts of Ami3. A strain carrying an aTc-inducible copy of *ami3* was grown in the indicated concentrations of aTc for two hours. Cell lysate was analyzed by Western blotting using anti-Strep and anti-RpoB as a loading control. **B. Ami3-mRFP localization.** Ami3-mRFP was expressed under an aTc-inducible promoter on an episomal vector in either wild-type or Δ*pmt* cells. Strains were analyzed by microscopy after 2 hours of induction with 100 ng/mL aTc. The localization of Ami3-mRFP to the poles, mid-cell, or bulges was quantified for both strains. In some cases, cells did not exhibit clear Ami3-mRFP localization; these were marked as "None." 100 cells were counted in each strain. **C. Catalytic mutants of Ami3 accumulate to varying degrees.** Whole cell lysate of the indicated strains was analyzed by Western blotting using anti-Strep and anti-RpoB as a loading control. Ami3* indicates the respective Ami3 allele. **D. Killing dynamics of Ami3 overexpression in different HtrA genetic backgrounds.** Left: Strains expressing either wild-type *htrA* or *htrA(S354A)* and *ami3* under an aTc-inducible episomal construct were grown in the presence or absence of 100 ng/mL aTc. Aliquots were taken at the indicated time points for CFU analysis. *p<0.05, **p<0.01. Error bars represent standard deviation of the mean. Right: the aTc MIC of strains expressing either wild-type *htrA* or *htrA(S354A)* and *ami3* under an aTc-inducible episomal construct was measured at two different temperatures. Western blot images were cropped, but display all relevant lanes and reactive bands.

Figure S4

A.

Background	Total Peptides	Unique Peptides
Wild type	1400	62
Δ*pmt*	1524	60

Residue	XCorr	ΔCorr	# Ions	Peptide	Max	PPM
T122	1.284	0.314	15/84	R.T#NTVQIAITRPENAAPTAPAPK.N	2.01E+05	0.44
T130	2.324	0.018	25/84	R.TNTVQIAIT#RPENAAPTAPAPK.N	1.73E+07	-0.4
T138	2.139	0.265	23/84	R.TNTVQIAITRPENAAPT#APAPK.N	1.73E+07	-0.57
T138	3.164	0.406	27/84	R.TNTVQIAITRPENAAPT#APAPK.N	1.73E+07	-0.41

B.

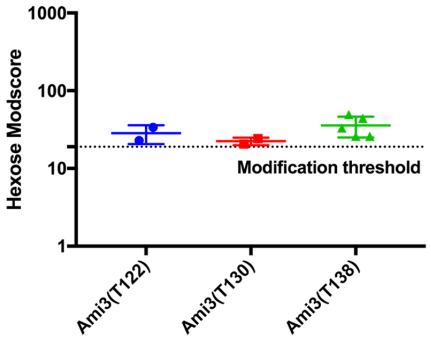

C.

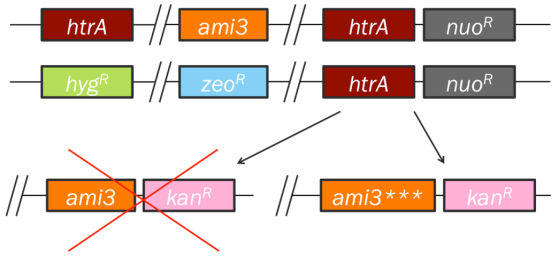

	Swap	Double integration
Wild type	0	60
T122A	0	60
T130A	0	60
T138A	0	60
T122A/T130A	33	27
T122A/T138A	0	60
T130A/T138A	0	60
T122A/T130A/T138A	26	34

D.

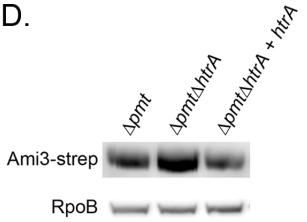

Figure S4, related to Figure 5: Ami3 is mannosylated. A. Hexose modified peptides of Ami3. Ami3-Strep was immunoprecipitated from wild-type and Δ*pmt* backgrounds and analyzed by mass spectrometry for hexose modifications. Total peptides and unique peptides from each strain's samples are listed. Only the wild-type sample yielded modifications, which are scored below. **B. Hexose modification scores of Ami3.** Scores over 19 signify a confident assignment of modification. **C. Toxicity of Ami3 mannosylation mutants.** Top: the endogenous copies of *ami3* and *htrA* were replaced with zeocin and hygromycin resistance cassettes, respectively, and a copy of *htrA* was integrated at the L5 site. *ami3* or mannosylation mutant alleles of *ami3* (*ami3****) were transformed into this background. Full swaps that acquire kanamycin resistance at the expense of noursethricin resistance render strains devoid of *htrA* and must thus carry a suppressor mutation. Bottom: quantification of *ami3* and *ami3**** swaps. A total of 60 transformants were tested for antibiotic resistance. **C. Ami3 stability is still dependent on HtrA in the absence of Pmt.** Whole cell lysate of the indicated strains was analyzed by Western blotting using anti-Strep and anti-RpoB as a loading control. Western blot images were cropped, but display all relevant lanes and reactive bands.

Figure S5

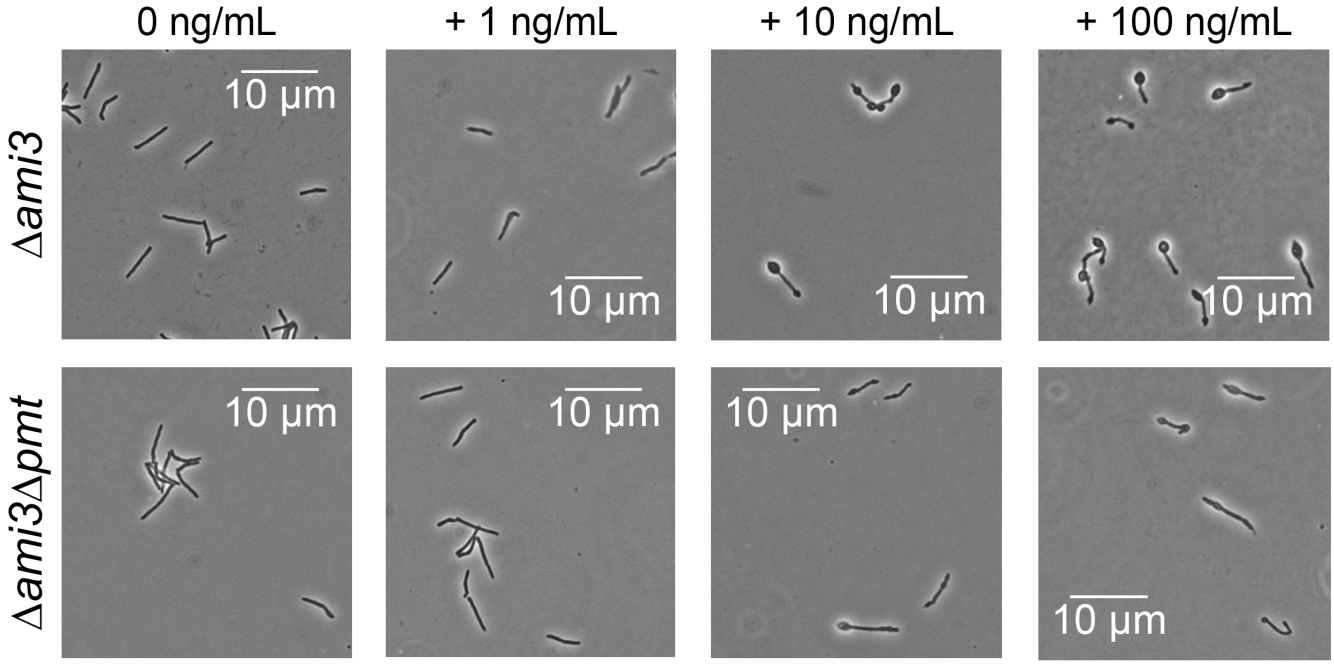

Figure S5, related to Figure 6: Loss of *pmt* relieves morphological defects in Ami3 overexpressions in a dose-dependent manner. Strains expressing *ami3* in a wild-type or Δ*pmt* background under an aTc-inducible promoter were grown in the indicated concentrations of aTc.

Figure S6

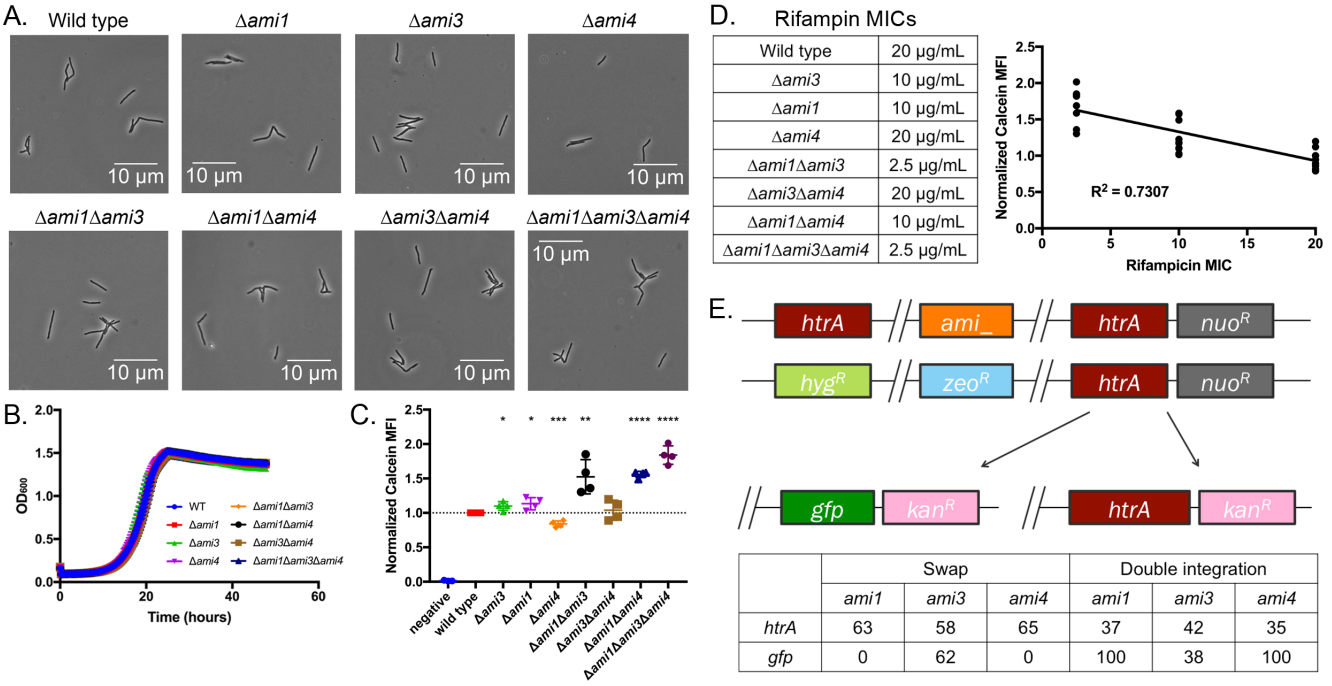

Wild type	20 μg/mL
Δ*ami3*	10 μg/mL
Δ*ami1*	10 μg/mL
Δ*ami4*	20 μg/mL
Δ*ami1*Δ*ami3*	2.5 μg/mL
Δ*ami3*Δ*ami4*	20 μg/mL
Δ*ami1*Δ*ami4*	10 μg/mL
Δ*ami1*Δ*ami3*Δ*ami4*	2.5 μg/mL

	Swap			Double integration		
	ami1	*ami3*	*ami4*	*ami1*	*ami3*	*ami4*
htrA	63	58	65	37	42	35
gfp	0	62	0	100	38	100

Figure S6, related to Figure 2: Ami1, Ami3, and Ami4 contribute to cell wall impermeability. A and B. Single and combinatorial knockouts of *ami1, ami3,* and *ami4* grow normally. The indicated strains were grown to log phase and observed by microscopy, or grown at 37°C. Error bars represent standard deviation of the mean. **C and D. Combinatorial amidase knockouts exhibit increased permeability to calcein and rifampin.** The indicated strains were grown in the presence of calcein or rifampin; calcein permeability and rifampin MIC are negatively correlated. Calcein mean fluorescence intensity (MFI) was measured by flow cytometry and normalized to wild type. *p<0.05, **p<0.01, ***p<0.001, ****p<0.0001. Error bars represent standard deviation of the mean. **E. Knocking out *ami3,* but not *ami1* or *ami4*, suppresses *htrA* essentiality.** Top: the endogenous copies of the indicated amidase allele and *htrA* were replaced with zeocin and hygromycin resistance cassettes, respectively, and a copy of *htrA* was integrated at the L5 site. *htrA* or *gfp* were transformed into this background. Full swaps that acquire kanamycin resistance at the expense of noursethricin resistance render strains devoid of *htrA* and must thus carry a suppressor mutation. Bottom: quantification of amidase suppressor swaps. A total of 100 transformants were tested for antibiotic resistance.